Hamiltonian analysis of transverse beam dynamics in high-brightness photoinjectors

Chun-xi Wang*
Argonne National Laboratory, 9700 South Cass Avenue, Argonne, Illinois 60439, USA
(Received 5 October 2005; published 23 October 2006)

A general Hamiltonian suitable for perturbative analysis of rapidly accelerating beams is derived from first principles. With the proper choice of coordinates, the resulting Hamiltonian has a simple and familiar form, yet is able to take into account the rapid acceleration, rf focusing, magnetic focusing, and average space-charge forces in rf photoinjectors. From the linear Hamiltonian, the beam-envelope evolution is solved and analyzed, which better illuminates the invariant-envelope solution as well as the theory of emittance compensation. The third-order nonlinear Hamiltonian is derived and analyzed to some extent. To make the analysis systematic and self-contained, alternative derivations are given for the smoothed ponderomotive rf focusing and the transfer matrix of a rf cavity.

DOI: 10.1103/PhysRevE.74.046502 PACS number(s): 29.27.Bd, 41.75.−i, 41.85.−p, 29.25.Bx

I. INTRODUCTION

High-brightness rf photoinjectors have become the premier electron source for applications that demand high-brightness and high-intensity electron beams, such as free-electron lasers based on self-amplified spontaneous emission. A key advance in rf photoinjector development is the so-called emittance compensation, which brings under control the correlated transverse emittance growth due to linear space-charge forces [1,2]. Beam dynamics in rf photoinjectors is rather complex because of the strong collective space-charge forces and time-dependent rf forces that electrons experience while being rapidly accelerated from rest to relativistic velocities. Although most of the design studies are based on simulations, many theoretical investigations have been done to better understand the dynamics. Besides the pioneering analysis leading to the proposal of (space-charge) emittance compensation [1], two well-known analyses are representative: one is based on analytical integration of the single-particle equation of motion [3], and the other is based on analysis of the beam-envelope equation [4]. The former provides critical insights during the early days of development, while the latter provides a comprehensive account of emittance compensation with the introduction of the invariant-envelope solution. However, improvement is desirable for better understanding and treatment of the physics. Here a fresh investigation is presented based on a Hamiltonian analysis of the system. The goal is to establish a rigorous framework for systematically studying the dynamics, which can yield and improve established results, and, furthermore, lay the groundwork for analyzing dynamics beyond the linear dynamics covered by the transverse envelope equation. The Hamiltonian we derived is suitable for six-dimensional treatment. However, our present analysis neglects longitudinal dynamics and is limited to the third-order Hamiltonian.

The Hamiltonian approach has been used extensively in perturbative analysis of circular machines, especially for analyzing nonlinearity. However, it is seldom used in accelerators with rapid acceleration. Consequently, commonly used Hamiltonians assume a reference particle with (quasi)constant momentum, which is not suitable for our purpose. Thus, in Sec. II, starting from the very basic relativistic Hamiltonian for a single particle, we derive a generic Hamiltonian with an accelerating reference particle. With the proper choice of coordinates, the resulting Hamiltonian has a simple and familiar form, yet is able to take into account the rapid acceleration, rf focusing, magnetic focusing, and average space-charge forces in a rf photoinjector. This section is independent of the rest of the paper, and the result should also be of interest to systems other than photoinjectors.

Section III specifies the general electromagnetic fields encountered in rf photoinjectors and the explicit field models used in our analysis. The second-order Hamiltonian is derived with these fields. Then linear focusing forces and commonly used approximations are addressed. Unique to the choice of accelerating coordinates, there is a pseudofocusing force in addition to the Lorentz forces, which helps to significantly reduce the complication due to acceleration. Subtle cancellation between Lorentz focusing and pseudofocusing is revealed. Smoothed rf focusing is derived in the reduced coordinates.

Section IV analyzes the beam-envelope equation resulting from the linear Hamiltonian. Our treatment of the invariant-envelope solution is much simpler and provides a more satisfactory physical picture. A general solution for small oscillations around the invariant envelopes is given, which resembles the solution of the simple "illustrative model" in [4]. For analyzing split photoinjectors, the beam envelope in drift space is discussed and a better approximation to the beam-spreading curve is given.

Section V discusses the emittance oscillation based on the envelope solutions, with emphasis more on the physics of the invariant envelope and emittance compensation. A practical matching condition is readily established, as well as the crossover energy from the space-charge-dominated laminar regime to the emittance-dominated thermal regime. A general proof is given for the damping of correlated emittance when a beam evolves close to invariant envelopes. The "double-minimum" feature of emittance oscillation in drift space of a split injector is explained simply by beam spreading due to space charge.

*Electronic address: wangcx@aps.anl.gov

For those not interested in Hamiltonian analysis, Secs. IV and V can be read without understanding the others. They provide an improved account of the essential part of emittance compensation theory [4].

In Sec. VI, the third-order Hamiltonian is analyzed for emittance-compensated photoinjectors. The chromatic effect due to energy spread and the geometric effect due to the rf field are discussed based on preliminary treatments of these nonlinearities.

As related exercises, alternative derivations (consistent with our analysis) are given in the appendixes for the smoothed ponderomotive rf focusing published in [5] and the transfer matrix of a rf cavity published in [6]. Other extensive appendixes are included so that the derivations in the text can be followed with ease.

II. HAMILTONIANS WITH AN ACCELERATING REFERENCE PARTICLE

The Hamiltonians commonly used for studying beam dynamics in accelerators assume a reference particle with (quasi)constant momentum. In rf injectors, electrons are rapidly accelerated; thus a Hamiltonian with an accelerating reference particle is needed for perturbative analysis. Here we start from the well-known relativistic Hamiltonian for a particle of mass m and charge q moving under the influence of an external electromagnetic field, i.e.,

$$H = q\phi(\mathbf{X},t) + \sqrt{m^2c^4 + [\mathbf{P} - q\mathbf{A}(\mathbf{X},t)]^2c^2}, \tag{1}$$

where $\mathbf{X}$ is the laboratory-frame Cartesian coordinate of the particle and $\mathbf{P}$ is the canonical momentum. The electromagnetic field is given by the scalar potential ϕ and vector potential $\mathbf{A}$. Time t is the independent variable.

For convenience we use the longitudinal position s of a reference particle as the independent variable and replace t with the time of the reference particle $t_r(s)$. Furthermore, we normalize the momentum by mc. In other words, we use $\hat{\mathbf{X}}(s)=\mathbf{X}(t_r)$ and $\hat{\mathbf{P}}(s)=\mathbf{P}(t_r)/mc$ as the canonical variables. The new Hamiltonian is given by

$$\hat{H}(\hat{\mathbf{X}},\hat{\mathbf{P}},s) = \frac{1}{ds/dt_r}\frac{H}{mc} = \frac{H(\mathbf{X},\mathbf{P},t_r(s))}{\beta_r(s)mc^2}. \tag{2}$$

It is clear that $\hat{H}(\hat{\mathbf{X}},\hat{\mathbf{P}},s)$ yields the same Hamiltonian equations as $H(\mathbf{X},\mathbf{P},t)$ does. Note that we do not change t to a canonical variable in order to preserve it as the underlying independent variable so that particle positions are evaluated at the same time, which is important for evaluating space-charge forces. Using the normalized electromagnetic field potentials

$$\hat{\phi} = \frac{q\phi}{mc^2}, \quad \hat{\mathbf{A}} = \frac{q\mathbf{A}}{mc}, \tag{3}$$

the Hamiltonian simply reads

$$\hat{H} = \frac{1}{\beta_r}\hat{\phi} + \frac{1}{\beta_r}\sqrt{1 + [\hat{\mathbf{P}} - \hat{\mathbf{A}}]^2}. \tag{4}$$

Before continuing, let us say a few words about our notation scheme. Subscripts and superscripts in Roman font are descriptive in nature. For examples, "k" refers to kinetic (vs canonical), "r" refers to the reference particle, "sc" refers to space charge, and "rf" refers to rf field. On the other hand, subscripts in italic font usually relate to a component of coordinates, such as x, y, z, and s. It is subtle to distinguish the radial-component subscript "r" from the reference-particle subscript "r". Fortunately, it is quite obvious in most cases, and few cases may have to rely on the difference in font. A caret usually indicates a normalized quantity, which is often dimensionless, such as $\hat{\mathbf{P}}$, $\hat{\phi}$, and $\hat{\mathbf{A}}$, but not always, such as $\hat{\mathbf{X}}$ and the reduced coordinates $\hat{x}$ and $\hat{\sigma}$ used later.

To facilitate perturbative treatment of beam dynamics, we change variables to the deviations from the reference particle with the new coordinate $\mathbf{x}=\hat{\mathbf{X}}-\hat{\mathbf{X}}_r=\mathbf{X}-\mathbf{X}_r$ and the new momentum $\mathbf{p}=\hat{\mathbf{P}}-\hat{\mathbf{P}}_r=(\mathbf{P}-\mathbf{P}_r)/mc$. Using the generating function $F_2(\hat{\mathbf{X}},\mathbf{p},s)=(\hat{\mathbf{X}}-\hat{\mathbf{X}}_r)\cdot(\mathbf{p}+\hat{\mathbf{P}}_r)$, the new Hamiltonian becomes

$$H(\mathbf{x},\mathbf{p},s) = \frac{1}{\beta_r}\hat{\phi} + \frac{1}{\beta_r}\sqrt{1 + [\mathbf{p} + \hat{\mathbf{P}}_r - \hat{\mathbf{A}}]^2} - \mathbf{X}_r'\cdot(\mathbf{p} + \hat{\mathbf{P}}_r) + \mathbf{x}\cdot\hat{\mathbf{P}}_r', \tag{5}$$

where the prime means differentiation with respect to s. Since several canonical transformations are used in this paper, we choose not to introduce new symbols for new Hamiltonians, which can be distinguished by their canonical coordinates.

To expand the square root in the Hamiltonian into a series, we note that $\hat{\mathbf{P}}_r-\hat{\mathbf{A}}=\hat{\mathbf{P}}_r^k-\Delta\hat{\mathbf{A}}$, where $\hat{\mathbf{P}}_r^k$ is the dimensionless kinetic momentum of the reference particle, and $\Delta\hat{\mathbf{A}}\equiv\hat{\mathbf{A}}-\hat{\mathbf{A}}_r$ is the difference in vector potential experinced by a particle and the reference particle, which should be small. Thus the terms under the square root can be written as $1+(\hat{P}_r^k)^2+2\hat{\mathbf{P}}_r^k\cdot(\mathbf{p}-\Delta\hat{\mathbf{A}})+(\mathbf{p}-\Delta\hat{\mathbf{A}})^2$, where $\hat{P}_r^k=\beta_r\gamma_r$ is the magnitude of $\hat{\mathbf{P}}_r^k$. The first two terms are dominating and sum to γ_r^2. Taking γ_r^2 out of the square root, the rest becomes $1+2\beta_r^2\boldsymbol{\delta}_z+\beta_r^2\boldsymbol{\delta}^2$, where

$$\boldsymbol{\delta} = \frac{\mathbf{p} - \Delta\hat{\mathbf{A}}}{\hat{P}_r^k} = \frac{\mathbf{P}^k - \mathbf{P}_r^k}{P_r^k} \tag{6}$$

is the relative deviation in kinematic momentum, and the subscript z indicates the longitudinal component in the direction of $\mathbf{P}_r^k$. This form is suitable for Taylor expansion since both $\mathbf{p}/\hat{P}_r^k$ and $\Delta\hat{\mathbf{A}}/\hat{P}_r^k$, and thus $\boldsymbol{\delta}$, are small quantities. Furthermore, when the momentum of the reference particle is not much larger than the momentum deviation, i.e., $\boldsymbol{\delta}$ is not small, β_r will be small. Expanding the square-root term up to the third order yields $1+\beta_r^2\boldsymbol{\delta}_z+\beta_r^2(\boldsymbol{\delta}^2-\beta_r^2\boldsymbol{\delta}_z^2)/2-\beta_r^4\boldsymbol{\delta}_z(\boldsymbol{\delta}^2-\beta_r^2\boldsymbol{\delta}_z^2)/2+O(\boldsymbol{\delta}^4)$. Now the Hamiltonian can be expanded as

$$H = \frac{\gamma_r}{\beta_r} - \mathbf{X}_r' \cdot \hat{\mathbf{P}}_r + \frac{1}{\beta_r}\hat{\phi} + \hat{\mathbf{P}}_r' \cdot \mathbf{x} - \mathbf{X}_r' \cdot \mathbf{p} + \hat{\mathbf{P}}_r^k \cdot \boldsymbol{\delta} + \frac{\hat{P}_r^k}{2}\left(\boldsymbol{\delta}_\perp^2 + \frac{1}{\gamma_r^2}\boldsymbol{\delta}_z^2\right) - \frac{\beta_r^2}{2}\hat{\mathbf{P}}_r^k \cdot \boldsymbol{\delta}\left(\boldsymbol{\delta}_\perp^2 + \frac{1}{\gamma_r^2}\boldsymbol{\delta}_z^2\right) + \cdots . \tag{7}$$

Ignoring both the zeroth-order terms, which do not play a role in the Hamiltonian equations, and the first-order terms, which cancel out since the reference particle follows the first-order solution (Appendix A), the Hamiltonian reduces to $H=H_2+H_3+\cdots$, where

$$H_2 = \left(\frac{1}{\beta_r}\hat{\phi} - \hat{A}_z\right)_2 + \frac{\hat{P}_r^k}{2}\left(\boldsymbol{\delta}_\perp^2 + \frac{1}{\gamma_r^2}\boldsymbol{\delta}_z^2\right)_2, \tag{8}$$

$$H_3 = \left(\frac{1}{\beta_r}\hat{\phi} - \hat{A}_z\right)_3 + \frac{\hat{P}_r^k}{2}\left(\boldsymbol{\delta}_\perp^2 + \frac{1}{\gamma_r^2}\boldsymbol{\delta}_z^2\right)_3 - \frac{\beta_r^2}{2}(\hat{\mathbf{P}}_r^k \cdot \boldsymbol{\delta}_1)\left(\boldsymbol{\delta}_\perp^2 + \frac{1}{\gamma_r^2}\boldsymbol{\delta}_z^2\right)_2 . \tag{9}$$

Hereafter integer subscripts indicate which order to keep. Note that the first terms in both expressions are potential terms depending only on the coordinates.

The internal space-charge force is modeled by an average static potential ϕ_0^{sc} in the beam frame (of the reference particle moving in z direction), assuming the particles' relative motions are negligible for evaluating the space-charge force. Transforming to the laboratory frame, we have

$$\phi^{sc} = \gamma_r \phi_0^{sc}, \quad A_z^{sc} = \frac{\beta_r}{c}\phi^{sc}, \tag{10}$$

i.e.,

$$\hat{A}_z^{sc} = \beta_r \hat{\phi}^{sc} = \beta_r \gamma_r \hat{\phi}_0^{sc}. \tag{11}$$

Using these relations, the space-charge contribution to the potential terms $\hat{\phi}/\beta_r - \hat{A}_z$ in the Hamiltonian reduces to $\hat{\phi}_0^{sc}/\beta_r\gamma_r$, showing the well-known suppression of space-charge force due to cancellation of its electric and magnetic forces in the ultrarelativistic limit. However, the space-charge vector potential also contributes to the kinematic terms via $\boldsymbol{\delta}$, whose effects are not canceled at all and may play a role even in the ultrarelativistic limit (for examples, see Sec. VI and [7]).

The second-order Hamiltonian H_2 governs the linear focusing properties around the reference orbit and usually dominates the dynamics. It depends on the linear order $\boldsymbol{\delta}$, which is $[\mathbf{p} - (\mathbf{x}\cdot\nabla\hat{\mathbf{A}})_r]/\hat{P}_r^k$. To simplify the linear dynamics, we make a linear canonical transformation generated by

$$F_2 = x\left(\sqrt{\hat{P}_r^k}\,\hat{p}_x - \frac{1}{2}\sqrt{\hat{P}_r^k}\sqrt{\hat{P}_r^k}'\,x + \frac{1}{2}(\partial_x \hat{A}_x)_r\, x\right) + (x \leftrightarrow y) + z\left(\hat{p}_z + \frac{1}{2}(\partial_z \hat{A}_z)_r\, z\right). \tag{12}$$

The variables are transformed as

$$\hat{x} = \sqrt{\hat{P}_r^k}\,x = \sqrt{\beta_r\gamma_r}\,x, \tag{13a}$$

$$p_x = \sqrt{\hat{P}_r^k}\,\hat{p}_x - \sqrt{\hat{P}_r^k}'\,\hat{x} + \frac{(\partial_x \hat{A}_x)_r}{\sqrt{\hat{P}_r^k}}\hat{x}, \tag{13b}$$

$$\hat{z} = z, \tag{13c}$$

$$p_z = \hat{p}_z + (\partial_z \hat{A}_z)_r\,\hat{z}, \tag{13d}$$

and the y dimension is similarly transformed. Note that $\hat{x}$ and $\hat{y}$ are the so-called reduced coordinates [8,9]. Under the anticipated conditions for the vector potential

$$(\partial_z A_\perp)_r = 0 \quad \text{and} \quad (\partial_y A_x)_r = -(\partial_x A_y)_r, \tag{14}$$

the new Hamiltonian reduces to (Appendix A)

$$H_2 = \left(\frac{1}{\beta_r}\hat{\phi} - \hat{A}_z\right)_2 + \frac{\hat{p}_x^2}{2} + \left[-\frac{\sqrt{\hat{P}_r^k}''}{\sqrt{\hat{P}_r^k}} + \frac{1}{\hat{P}_r^k}\frac{\partial^2 \hat{A}_x}{\partial s \partial x}\right|_r + \left(\frac{\partial_x \hat{A}_y}{\hat{P}_r^k}\right)_r^2\Bigg]\frac{\hat{x}^2}{2} + (x \leftrightarrow y \text{ in the previous two terms}) + \left(\frac{\partial_y \hat{A}_x}{\hat{P}_r^k}\right)_r(\hat{x}\hat{p}_y - \hat{y}\hat{p}_x) + \frac{1}{2\beta_r^2\gamma_r^4}(\hat{\mathbf{x}}_\perp \cdot \nabla_\perp \hat{A}_z)_r^2 + \frac{\hat{p}_z^2}{2\beta_r\gamma_r^3} - \frac{\hat{p}_z}{\beta_r\gamma_r^3}(\mathbf{x}_\perp \cdot \nabla_\perp \hat{A}_z)_r + \left.\frac{\partial^2 \hat{A}_z}{\partial s \partial z}\right|_r \frac{\hat{z}^2}{2}. \tag{15}$$

The advantages of this transformation become clear now. The complication due to acceleration is reduced to a pseudo-focusing. The kinematic and potential terms are separated, and the Hamiltonian resumes a familiar form. Note that, until now, the treatment is generally valid under the conditions in Eq. (14).

The third-order Hamiltonian can be worked out using the reduced coordinates as (Appendix A)

$$H_3 = H_C + H_G + H_L. \tag{16}$$

The chromatic part reads

$$H_C = -\frac{\beta_r}{2\gamma_r}\hat{p}_z[(\hat{p}_x^2 + \hat{p}_y^2) + w_c(\hat{x}^2 + \hat{y}^2)] + \frac{1}{\gamma_r^2}\hat{p}_z\left(\frac{(\hat{P}_r^k)'}{2}(\hat{x}\hat{p}_x + \hat{y}\hat{p}_y) - (\partial_y \hat{A}_x)_r(\hat{x}\hat{p}_y - \hat{y}\hat{p}_x)\right),$$

where

$$w_c = \left(\frac{\sqrt{\hat{P}_r^k}'}{\sqrt{\hat{P}_r^k}}\right)^2 + \left(\frac{\partial_x \hat{A}_y}{\hat{P}_r^k}\right)_r^2 + \frac{(\partial_r^2 \hat{A}_z)_r}{(\hat{P}_r^k)^3}.$$

The geometric part reads

$$H_G = \frac{1}{\hat{P}_r^k}\left[(\hat{\phi}_0^{sc})_3 + w_g\frac{(\hat{x}^2 + \hat{y}^2)\hat{z}}{2} - \left(\frac{\partial^2 \hat{A}_r}{\partial z \partial r}\right)_r(\hat{x}\hat{p}_x + \hat{y}\hat{p}_y)\hat{z}\right],$$

where

$$w_g = \frac{(\hat{P}_r^k)'}{\hat{P}_r^k}\left(\frac{\partial^2 \hat{A}_r}{\partial z \partial r}\right)_r - \left(\frac{\partial^3 \hat{A}_z^{rf}}{\partial z \partial r^2}\right)_r.$$

The longitudinal part reads

$$H_L = -\frac{\hat{p}_z^3}{2\gamma_r^4} - \frac{1}{2\beta_r\gamma_r^3}(\partial_z^2 \hat{A}_z)_r \hat{z}^2 \hat{p}_z - \left(\partial_z^3 \hat{A}_z^{rf}\right)_r \frac{\hat{z}^3}{6}.$$

Note that this third-order Hamiltonian was derived with the fields in the next section in mind. Clearly all terms are rotationally invariant since we have considered only axisymmetric fields.

III. LINEAR FOCUSING AND HAMILTONIAN

In rf photoinjectors there is no dipole field, thus the reference orbit is straight and $(\nabla_\perp A_z)_r = 0$. The external field typically consists of an axisymmetric TM_{01} rf accelerating field with vector potential (using the real part)

$$A_z^{rf} = \mathsf{E}_0 \sum_{n=-\infty}^{\infty} \frac{a_n}{\omega} J_0(k_{rn} r) e^{i[\omega t - k_{zn}(s+z)+\varphi_0]}, \tag{17a}$$

$$A_r^{rf} = i\mathsf{E}_0 \sum_{n=-\infty}^{\infty} \frac{k_{zn}}{k_{rn}} \frac{a_n}{\omega} J_1(k_{rn} r) e^{i[\omega t - k_{zn}(s+z)+\varphi_0]}, \tag{17b}$$

and solenoid focusing field

$$\hat{\mathbf{A}}^{mag} = (-\hat{b}_s y, \hat{b}_s x, 0). \tag{18}$$

Here E_n is the amplitude of the space harmonic of index n and $a_n = \mathsf{E}_n/\mathsf{E}_0$; ω is the rf frequency, and φ_0 is the initial rf phase from the zero crossing at the origin (the same convention as in [3,4]). The longitudinal and transverse wave numbers of the nth space harmonic (k_{zn} and k_{rn}, respectively) are given by $k_{zn} = k_{z0} + 2\pi n/d$ and $k_{rn}^2 + k_{zn}^2 = k^2 = (\omega/c)^2$, where d is the period of the rf structure. J_0 and J_1 are the Bessel functions, and r is the radial coordinate. $\hat{b}_s = (q/2mc) B_s(0,0,s)$ is the normalized solenoid strength.

Generally the space-charge potential can be complicated. Here we assume an axisymmetric bunch of charge Q, centered at the reference particle, whose potential can be written as (Appendix B)

$$\phi_0^{sc} = -\frac{Q}{4\pi\varepsilon_0\sqrt{2\pi}\gamma_r\sigma_z}\left(g_0 + g\frac{x^2+y^2}{2\sigma_r^2}\right) + O(X^4), \tag{19}$$

where σ_r and σ_z are the transverse and longitudinal beam sizes whose evolutions need to be determined. $\gamma_r\sigma_z$ is the bunch length in the beam frame, and $g_0(z)$ and $g(z)$ are geometric form factors that change with time. Since the space-charge force may have strong nonlinear dependence on z that may be considered as a parameter in many treatments, we do not expand the form factors here.

Inserting these fields into Eq. (15), the linear Hamiltonian becomes

$$H_2 = \frac{\hat{p}_x^2 + \hat{p}_y^2}{2} + K\frac{\hat{x}^2 + \hat{y}^2}{2} - \frac{\hat{b}_s}{\hat{P}_r^k}(\hat{x}\hat{p}_y - \hat{y}\hat{p}_x) + \frac{\hat{p}_z^2}{2\beta_r\gamma_r^3} + \left(\frac{\partial^2 \hat{A}_z}{\partial s \partial z} - \frac{\partial^2 \hat{A}_z^{rf}}{\partial z^2} + \frac{1}{\hat{P}_r^k}\partial_z^2 \hat{\phi}_0^{sc}\right)_r \frac{\hat{z}^2}{2}, \tag{20}$$

where the transverse focusing strength K is given by

$$K(z,s) = -\frac{\sqrt{\hat{P}_r^k}''}{\sqrt{\hat{P}_r^k}} + \frac{1}{\hat{P}_r^k}(\partial_s \partial_r \hat{A}_r^{rf} - \partial_r^2 \hat{A}_z^{rf})_r + \left(\frac{\hat{b}_s}{\hat{P}_r^k}\right)^2 + \frac{1}{(\hat{P}_r^k)^2}\partial_x^2 \hat{\phi}_0^{sc}|_{r=0}. \tag{21}$$

Note that the two transverse planes are coupled by the solenoid through the angular momentum term. This coupling can be removed by transforming to the Larmor frame that rotates at one-half of the cyclotron frequency. Such a rotation leaves all other terms unchanged due to cylindrical symmetry. Hereafter, the angular momentum term will be dropped with the understanding that the dynamical variables refer to the Larmor frame. Also note that the focusing strength K depends on z in addition to s through the space-charge form factor $g(z,s)$. The transverse and longitudinal motions are further coupled implicitly through the bunch sizes.

The rf field contributes the first two terms of the focusing strength in Eq. (21). The first one is a pseudofocusing resulting from longitudinal acceleration. The second one is due to the transverse Lorentz force F_r and is equal to $-(\partial_r F_r)_r/\beta_r^2\gamma_r mc^2$ (Appendix C). The average Lorentz force has been studied [5,6] and referred to as "ponderomotive focusing." However, in the reduced coordinates, the Lorentz focusing is surprisingly canceled by the γ_r'' term from the pseudofocusing, which can be written as

$$-\frac{\sqrt{\hat{P}_r^k}''}{\sqrt{\hat{P}_r^k}} = \frac{1}{4}\left(1 + \frac{2}{\gamma_r^2}\right)\left(\frac{\gamma_r'}{\beta_r^2\gamma_r}\right)^2 - \frac{\gamma_r''}{2\beta_r^2\gamma_r}. \tag{22}$$

For the reference particle we have

$$\gamma_r' = \hat{E}_z = \frac{q}{mc^2}E_z = -\frac{1}{c}\partial_t \hat{A}_z = \beta_r(\partial_z - \partial_s)\hat{A}_z \tag{23}$$

and (Appendix C)

$$\frac{\gamma_r''}{2\beta_r^2\gamma_r} = \frac{1}{\beta_r\gamma_r}(\partial_s \partial_r \hat{A}_r^{rf} - \partial_r^2 \hat{A}_z^{rf})_r + \frac{1}{2\beta_r^3\gamma_r^3 c}\partial_t \hat{E}_z. \tag{24}$$

The leading term cancels the transverse Lorentz focusing exactly. Thus the rf focusing strength in reduced coordinates can be written as

$$K^{rf} = \frac{\xi}{4\beta_r^2\gamma_r^2}\hat{E}_z^2 - \frac{1}{2\beta_r^3\gamma_r^3 c}\partial_t \hat{E}_z, \tag{25}$$

where $\xi = (1 + 2/\gamma_r^2)/\beta_r^2$, which quickly reduces to 1 as the reference particle becomes relativistic. This is the same as in Eq. (10) of [9].

Since the rf focusing may contain fast oscillations due to rf waves, one commonly used approximation is to smooth it out by averaging over a rf period. Note that such an average is in fact to smooth the Hamiltonian as one may expect. Assuming the changes (over a rf period) in β_r, γ_r, and accelerating rf phase φ_r are negligible, the average rf focusing can then be written as (Appendix C)

$$\bar{K}^{\mathrm{rf}} \simeq \frac{\xi}{4\beta_r^2\gamma_r^2}\left(\langle\gamma_r'\rangle^2 + \frac{\eta}{2}\hat{E}_0^2\right) - \frac{1}{2\beta_r^3\gamma_r^3}k\hat{E}_0\cos\varphi_r, \quad (26)$$

where the average acceleration gradient $\langle\gamma_r'\rangle = \hat{E}_0 \sin\varphi_r$, $\eta(\varphi_r) = \Sigma_{n=1}^{\infty}(a_n^2 + a_{-n}^2 - 2a_n a_{-n}\cos 2\varphi_r)$, and $\hat{E}_0 = q\mathsf{E}_0/mc^2$. The term containing η is the so-called ponderomotive focusing, reappearing from the averaged pseudofocusing as a result of $\langle\hat{E}_z^2\rangle - \langle\hat{E}_z\rangle^2$, the variance of the accelerating field. The last term in Eq. (26) is usually much smaller because there is an extra $1/\beta_r\gamma_r$ and furthermore the accelerating rf phase is close to $\pi/2$. Thus we will not consider this term further in this paper. Note that, with the smooth approximation, both β_r and γ_r should be smoothed quantities as well, as will be assumed in the following sections.

In summary, the total external focusing strength can be written as

$$K^{\mathrm{ext}} = \frac{\kappa}{\beta_r^2\gamma_r^2}, \quad (27)$$

where

$$\kappa(s) = \hat{b}_s^2 + \frac{\xi}{4}\hat{E}_z^2 - \frac{1}{2\beta_r\gamma_r c}\partial_t\hat{E}_z \simeq \left(\frac{qB_s}{2mc}\right)^2 + \langle\gamma_r'\rangle^2\left(\frac{1}{4} + \frac{\eta}{8\sin^2\varphi_r}\right), \quad (28)$$

respectively, from solenoid focusing and ponderomotive rf focusing. The approximation arises from the smooth operation with $\xi \simeq 1$. This approximate expression relates to the often-used Ω in [4] as

$$\kappa = \langle\gamma_r'\rangle^2\left(\Omega^2 + \frac{1}{4}\right), \quad \Omega^2 \equiv \frac{1}{\sin^2\varphi_r}\left[\frac{\eta}{8} + \left(\frac{B_s c}{E_0}\right)^2\right]. \quad (29)$$

Note that the approximations used in obtaining this result are suitable only when particles reach relativistic. After the smooth operation, $\kappa(s)$ is piecewise constant (neglecting fringe field).

The space-charge defocusing strength in Eq. (21) is

$$K^{\mathrm{sc}} = -\frac{qQg(z,s)}{4\pi\varepsilon_0\beta_r^2\gamma_r^3 mc^2\sqrt{2\pi}\sigma_z\sigma_r^2} = -\frac{2\kappa_s}{\beta_r^3\gamma_r^3\sigma_r^2}, \quad (30)$$

where the beam perveance $\kappa_s = Ig(s,z)/2I_A$, the peak current $I = \beta_r cQ/\sqrt{2\pi}\sigma_z$, and the Alfvén current $I_A = 4\pi\varepsilon_0 mc^3/q \simeq 17$ kA for electrons. Unlike the external focusing, the space-charge defocusing depends on the beam parameters and varies significantly along a bunch. A significant exception is a uniform ellipsoidal bunch for which the form factor g is independent of z (Appendix C).

IV. TRANSVERSE BEAM ENVELOPES

Ignoring the longitudinal dynamics in Eq. (20), the transverse dynamics of each z slice is governed by the simple Hamiltonian $(\hat{p}_x^2 + \hat{p}_y^2)/2 + K(s,z)(\hat{x}^2 + \hat{y}^2)/2$, whose behavior is well known, and the beam envelope can be described by the standard Courant-Snyder parameters with the β function satisfying [10] $\sqrt{\beta}'' + K\sqrt{\beta} - 1/\sqrt{\beta}^3 = 0$. The normalized emittance ϵ_n is conserved for each slice under this Hamiltonian. The rms beam size in the reduced variable is $\hat{\sigma} = \sqrt{\epsilon_n\beta} = \sqrt{\beta_r\gamma_r}\sigma$, where $\sigma = \sigma_r/\sqrt{2}$ represents either σ_x or σ_y. Using $\hat{\sigma}$, the β-function equation becomes the beam-envelope equation $\hat{\sigma}'' + K\hat{\sigma} - \epsilon_n^2/\hat{\sigma}^3 = 0$. Inserting the above focusing strength we have

$$\hat{\sigma}'' + \frac{\kappa}{\beta_r^2\gamma_r^2}\hat{\sigma} - \frac{\kappa_s}{\beta_r^2\gamma_r^2}\frac{1}{\hat{\sigma}} - \frac{\epsilon_n^2}{\hat{\sigma}^3} = 0. \quad (31)$$

This is the reduced beam-envelope equation [8], which is equivalent to the envelope equation commonly used in photoinjector studies [4]. However, the reduced envelope equation yields a more satisfactory physical picture [11].

For a space-charge-dominated beam, as in high-brightness photoinjectors, the emittance term can be neglected. When κ and κ_s are independent of s, an obvious solution of the reduced beam-envelope equation is given by $\hat{\sigma}'' = \hat{\sigma}' = 0$ and

$$\hat{\sigma} = \hat{\sigma}_{\mathrm{inv}} \equiv \sqrt{\frac{\kappa_s}{\kappa}} \simeq \sqrt{\frac{\kappa_s}{\left(\frac{qB_s}{2mc}\right)^2 + \langle\gamma_r'\rangle^2\left(\frac{1}{4} + \frac{\eta}{8\sin^2\varphi_r}\right)}}. \quad (32)$$

This is the so-called invariant envelope found obscurely in [4], which plays a critical role in the theory of emittance compensation in photoinjectors.

To better understand the dynamics governed by the reduced beam-envelope equation, we note that it can be obtained by an envelope Hamiltonian [12]

$$H(\hat{\sigma}, p_\sigma, s) = \frac{p_\sigma^2}{2} + V(\hat{\sigma}, s) \quad (33)$$

with a potential

$$V = \frac{\kappa}{\beta_r^2\gamma_r^2}\frac{\hat{\sigma}^2}{2} - \frac{\kappa_s}{\beta_r^2\gamma_r^2}\ln\frac{\hat{\sigma}}{\hat{\sigma}_{\mathrm{inv}}} + \frac{\epsilon_n^2}{2\hat{\sigma}^2}.$$

Introducing the parameter

$$\rho \equiv \left(\frac{\beta_r\gamma_r\epsilon_n}{\sqrt{\kappa_s}\hat{\sigma}_{\mathrm{inv}}}\right)^2 = \left(\frac{\beta_r\gamma_r\epsilon_n}{\kappa_s}\right)^2\kappa = \begin{cases} 0, & \text{space-charge dominated,} \\ \infty, & \text{emittance dominated,} \end{cases} \quad (34)$$

which is the ratio of the emittance term to the space-charge term (evaluated on the invariant envelope) in the envelope equation, we can write the potential V as

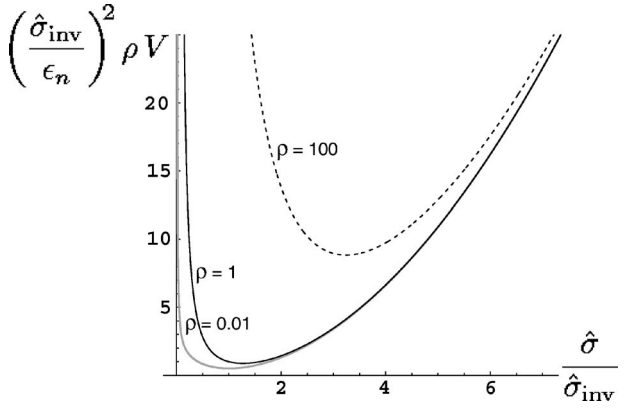

FIG. 1. Potential wells of the envelope Hamiltonian. The invariant envelope is at the bottom. Note that these curves correspond to ρV instead of V; thus the potential V actually is much higher in the laminar regime and decreases as ρ increases with beam energy.

$$V = \left(\frac{\epsilon_n}{\hat{\sigma}_{\rm inv}}\right)^2 \frac{1}{2\rho}\left(\frac{\hat{\sigma}^2}{\hat{\sigma}_{\rm inv}^2} - \ln\frac{\hat{\sigma}^2}{\hat{\sigma}_{\rm inv}^2} + \rho\frac{\hat{\sigma}_{\rm inv}^2}{\hat{\sigma}^2}\right). \tag{35}$$

The characteristics of this potential in different regimes are illustrated in Fig. 1. Solving $\partial_\sigma V=0$ gives the potential minimum at

$$\hat{\sigma}_\rho = \hat{\sigma}_{\rm inv}\sqrt{\frac{1}{2}+\sqrt{\frac{1}{4}+\rho}} = \begin{cases} \hat{\sigma}_{\rm inv}, & \rho \to 0, \\ \sqrt{\beta_{\rm r}\gamma_{\rm r}\epsilon_n/\sqrt{\kappa}}, & \rho \to \infty, \end{cases} \tag{36}$$

with a positive second derivative

$$\partial_\sigma^2 V(\hat{\sigma}_\rho) = \frac{\epsilon_n^2}{\rho\hat{\sigma}_{\rm inv}^4}\frac{4}{1+(1+4\rho)^{-1/2}} = \frac{\kappa}{\beta_{\rm r}^2\gamma_{\rm r}^2}\frac{4}{1+(1+4\rho)^{-1/2}}. \tag{37}$$

It is current independent in the regimes dominated by either space charge or emittance ($\rho\to 0$ or $\rho\to\infty$).

In the space-charge-dominated regime, $\rho \ll 1$, the invariant envelope is an equilibrium solution at the potential minimum. From the potential wells in Fig. 1, clearly the beam envelope will oscillate around the potential minimum provided that the parameter ρ does not change too rapidly. For small oscillations, the restoring force is given by Eq. (37) with $\rho=0$ for the space-charge-dominated regime. Let the deviation be $\delta\hat{\sigma}=\hat{\sigma}(z,s)-\hat{\sigma}_{\rm inv}$; the restoring force leads to

$$\delta\hat{\sigma}'' + \frac{2\kappa}{\beta_{\rm r}^2\gamma_{\rm r}^2}\delta\hat{\sigma} = 0. \tag{38}$$

With $\beta_{\rm r}\simeq 1$ and $\gamma_{\rm r}=\gamma_0+\gamma_{\rm r}'(s-s_0)$, the perturbative solution of the envelope equation around the invariant envelope can be written as (Appendix D)

$$\hat{\sigma} = \hat{\sigma}_{\rm inv} + \sqrt{\frac{\gamma_{\rm r}}{\gamma_0}}\frac{\delta\hat{\sigma}(0)}{\cos\theta}\cos(u+\theta), \tag{39a}$$

$$\hat{\sigma}' = -\sqrt{\frac{2\kappa}{\gamma_0\gamma_{\rm r}}}\frac{\delta\hat{\sigma}(0)}{\cos\theta}\sin(u+\theta-\theta_0). \tag{39b}$$

Here $u=\varpi\ln(\gamma_{\rm r}/\gamma_0)$ with $\varpi=\sqrt{2\kappa/\gamma_{\rm r}'^2-1/4}=\sqrt{2\Omega^2+1/4}$. The initial phase angles $\theta_0=\tan^{-1}(1/2\varpi)$ and $\theta=\tan^{-1}[1/2\varpi-\gamma_0\delta\hat{\sigma}'(0)/\varpi\gamma_{\rm r}'\delta\hat{\sigma}(0)]$. $\delta\hat{\sigma}(0)$ and $\delta\hat{\sigma}'(0)$ are the initial envelope deviations at s_0. Thanks to the reduced coordinates, this general solution resembles the no-acceleration result commonly used to illustrate emittance compensation [4]. In fact, the no-acceleration solution can be obtained from Eq. (39) by taking $\gamma_{\rm r}'\to 0$, $\gamma_{\rm r}=\gamma_0$, $u=\sqrt{2\kappa}\Delta s/\gamma_0$, $\theta_0=0$, and $\theta=-\tan^{-1}[\gamma_0\delta\hat{\sigma}'(0)/\sqrt{2\kappa}\delta\hat{\sigma}(0)]$. Note that $\delta\hat{\sigma}$ (thus $\delta\hat{\sigma}/\hat{\sigma}_{\rm inv}$) grows as $\sqrt{\gamma_{\rm r}}$, therefore this solution applies while $\gamma_{\rm r}/\gamma_0 \ll [\hat{\sigma}_{\rm inv}/\delta\hat{\sigma}(0)]^2\cos^2\theta$.

The existence of invariant envelopes requires external focusing to balance the space-charge defocusing. Thus, in free-drift regions, a special treatment is needed. The governing equation now is

$$\hat{\sigma}'' - \frac{\kappa_{\rm s}}{\beta_{\rm r}^2\gamma_{\rm r}^2}\frac{1}{\hat{\sigma}} = 0, \tag{40}$$

which can be normalized into the universal form

$$\tau'' - \frac{1}{\tau} = 0 \quad \text{with } \tau = \frac{\hat{\sigma}}{\sqrt{\kappa_{\rm s}}/\beta_{\rm r}\gamma_{\rm r}}, \tag{41}$$

assuming negligible perveance variations. From the envelope Hamiltonian, which is a constant of motion now, it is obvious that

$$\tau'^2 = \tau_0'^2 + 2\ln\frac{\tau}{\tau_0}, \tag{42}$$

where τ_0 and τ_0' are the initial values. The envelope can then be written as

$$\tau = \tau_0\exp\left(\frac{\tau'^2-\tau_0'^2}{2}\right) = \tau_{\rm w}e^{\tau'^2/2}, \tag{43}$$

which grows symmetrically away from a waist $\tau_{\rm w}=\tau_0 e^{-\tau_0'^2/2}$ located at $\tau'=0$. Equation (42) can be further integrated, using the waist as the origin for simplicity, as

$$\frac{\Delta s}{\sqrt{2}\tau_{\rm w}} = \pm\int_1^{\tau/\tau_{\rm w}}\frac{dx}{2\sqrt{\ln x}}, \tag{44}$$

which cannot be expressed with elementary functions. Approximate expressions can be obtained by expanding $1/\sqrt{\ln x}$ around $x=1$ and term-by-term integration, which gives $\sqrt{\tau/\tau_{\rm w}-1}+(1/12)(\tau/\tau_{\rm w}-1)^{3/2}+\cdots$. The leading term yields the familiar quadratic envelope [13]

$$\frac{\tau}{\tau_{\rm w}} \simeq 1 + \left(\frac{\Delta s}{\sqrt{2}\tau_{\rm w}}\right)^2. \tag{45}$$

A much better approximation can be obtained by keeping up to the second order of $\tau/\tau_{\rm w}-1$ in Δs^2, which yields

$$\frac{\tau}{\tau_w} \simeq 3\sqrt{1+\left(\frac{\Delta s}{\sqrt{3}\tau_w}\right)^2} - 2. \tag{46}$$

Setting $\Delta s = s - s_w$ with $s_w = \pm \tau_w \int_1^{\tau_0/\tau_w} dx/\sqrt{2\ln x} \simeq \pm \tau_w \sqrt{(\tau_0/\tau_w+2)^2/3 - 3}$, the origin shifts from the waist to arbitrary initial values τ_0 and τ_0', where the sign is chosen according to the opposite sign of τ_0'.

V. INVARIANT ENVELOPE AND LINEAR EMITTANCE COMPENSATION

Through the analysis of the beam-envelope Hamiltonian, we showed an (approximate) equilibrium solution and the evolution of nearby envelopes. Here we further emphasize the physical picture presented by these solutions and discuss the linear emittance compensation process in high-brightness photoinjectors.

Due to low thermal emittance from the photocathode and high charge, electrons evolve in the space-charge-dominated, quasilaminar regime [4], where $\rho \ll 1$ applies. For example, consider a beam accelerated near the crest in a standing-wave structure (thus $\eta \simeq 1$, $\sin\varphi_r \simeq 1$, $\Omega \simeq 1/8$, and $\kappa \simeq 3\gamma'^2/8$), the energy corresponding to $\rho = 1$ is given by

$$\beta_r\gamma_r = \frac{\kappa_s}{\epsilon_n\sqrt{\kappa}} \simeq \sqrt{\frac{8}{3}}\frac{\kappa_s}{\gamma'\epsilon_n}, \tag{47}$$

which is beyond a typical high-brightness photoinjector [4,14]. In the quasilaminar regime, there is a special exact solution of the nonlinear beam envelope equation, i.e., the invariant envelope $\hat{\sigma}_{inv}$ in Eq. (32). It is an equilibrium solution at the minimum of the envelope potential well. The (reduced) beam size is invariant as the beam propagates, and more importantly, the phase-space angle $\hat{\sigma}_{inv}'/\hat{\sigma}_{inv} = 0$ is invariant across beam slices with different perveance.

In the phase space of the reduced coordinates, the Twiss parameter $\alpha \propto \hat{\sigma}_{inv}' = 0$, i.e., the invariant envelope corresponds to an upright beam ellipse (with the long axis horizontal and the negligibly small short axis vertical, a line segment in the zero-emittance limit). In terms of single-particle motion, when a beam follows an invariant envelope, the net focusing strength $K = K^{ext} + K^{sc} = 0$, i.e., the defocusing linear space-charge force is canceled by the external focusing forces (including pseudofocusing due to acceleration). Thus all particles simply follow straight trajectories parallel to the beam axis (otherwise, the beam will diverge). In other words, the invariant envelope solution depicts the simplest laminar flow with straight flow lines parallel to the axis of propagation; clearly, a generalized Brillouin flow [15] for an accelerating beam.

Under linear (i.e., paraxial) approximation, the normalized emittance of each slice is conserved at a low value. However, due to different space-charge defocusing for different beam slices, each slice evolves differently starting from the same initial conditions at the cathode, which leads to a spread of phase-space orientations and thus a growth of the total emittance. The goal of emittance compensation is to adjust the conditions such that all slices are aligned again at a sufficiently high beam energy where space-charge forces are no longer important.

Since all invariant envelopes lie on the coordinate axis in phase space and stay aligned independent of slice currents, it is realized in [4] that the invariant envelope is the preferred mode to propagate a beam, and the desired condition for emittance compensation is to match all slices onto their invariant envelopes. However, due to perveance variation (except for a uniform ellipsoidal bunch), different slices may not be able to follow their invariant envelopes simultaneously; thus matching is done in a rms sense. Unmatched slices oscillate around their own invariant envelopes according to Eq. (39), i.e.,

$$\begin{bmatrix} \hat{\sigma} \\ \hat{\sigma}' \end{bmatrix} = \begin{bmatrix} \hat{\sigma}_{inv} \\ 0 \end{bmatrix} + R \begin{bmatrix} \delta\hat{\sigma}(0) \\ \delta\hat{\sigma}'(0) \end{bmatrix}, \tag{48}$$

where the transfer matrix R is given by Eq. (D6) with ϖ given by Eq. (D9). The emittance can be calculated as

$$\begin{aligned} \epsilon^2 = \langle\hat{\sigma}^2\rangle\langle\hat{\sigma}'^2\rangle - \langle\hat{\sigma}\hat{\sigma}'\rangle^2 &= \det\left(\left\langle \begin{bmatrix} \hat{\sigma} \\ \hat{\sigma}' \end{bmatrix} [\hat{\sigma}, \hat{\sigma}'] \right\rangle\right) \\ &= \det\left(\begin{bmatrix} \langle\delta\hat{\sigma}(0)^2\rangle & \langle\delta\hat{\sigma}(0)\delta\hat{\sigma}'(0)\rangle \\ \langle\delta\hat{\sigma}(0)\delta\hat{\sigma}'(0)\rangle & \langle\delta\hat{\sigma}'(0)^2\rangle \end{bmatrix} + \langle\hat{\sigma}_{inv}^2\rangle \right. \\ &\quad \times \begin{bmatrix} R_{22}^2 & -R_{21}R_{22} \\ -R_{21}R_{22} & R_{21}^2 \end{bmatrix} + \langle\hat{\sigma}_{inv}\delta\hat{\sigma}(0)\rangle \begin{bmatrix} 2R_{22} & -R_{21} \\ -R_{21} & 0 \end{bmatrix} \\ &\quad \left. + \langle\hat{\sigma}_{inv}\delta\hat{\sigma}'(0)\rangle \begin{bmatrix} 0 & R_{22} \\ R_{22} & -2R_{21} \end{bmatrix} \right), \end{aligned} \tag{49}$$

where the angular brackets mean averaging over the slices in a bunch. A more explicit expression can be obtained but the result is too messy to be interesting. However, it is important to note that only the R_{21} and R_{22} elements of the transfer matrix are involved and both are inversely proportional to $\sqrt{\gamma_r}$ and thus approach zero as the beam energy increases. Therefore, as long as all the slices propagate close to their invariant envelopes, the correlated emittance oscillations will be damped away and the emittance converges to an asymptotic value determined by the initial deviations from the invariant envelopes (the equilibrium), i.e.,

$$\epsilon \overset{\gamma_r\to\infty}{\to} \sqrt{\langle\delta\hat{\sigma}^2\rangle\langle\delta\hat{\sigma}'^2\rangle - \langle\delta\hat{\sigma}\delta\hat{\sigma}'\rangle^2}\Big|_{\gamma_r=\gamma_0}. \tag{50}$$

This is the minimum emittance a photoinjector may achieve ideally, assuming $\epsilon_n = 0$. Again, the critical condition in emittance compensation is that all the slices propagate close to their invariant envelopes with

$$\hat{\sigma}' = 0, \quad \text{i.e.,} \quad \frac{\sigma'}{\sigma} = -\frac{(\beta_r\gamma_r)'}{2\beta_r\gamma_r} \simeq -\frac{\gamma_r'}{2\gamma_r}. \tag{51}$$

Meanwhile, it is important to minimize $\delta\hat{\sigma}$ for all slices to reduce the magnitude of emittance oscillation and to ensure that all slices evolve close to their invariant envelopes.

As a concrete example, we consider the special case that all slices are aligned along $\hat{\sigma}' = 0$ initially; then $\delta\hat{\sigma}'(0) = 0$ and $\theta = \theta_0$ for all slices, and it is easy to see that

$$\epsilon = \sqrt{\langle \hat{\sigma}_{\rm inv}^2 \rangle \langle \delta\hat{\sigma}^2 \rangle - \langle \hat{\sigma}_{\rm inv} \delta\hat{\sigma} \rangle^2} |R_{21}| = \frac{\epsilon_0}{\sqrt{\gamma_{\rm r}}} \left| \sin\left(\varpi \ln \frac{\gamma_{\rm r}}{\gamma_0} \right) \right|, \tag{52}$$

where the constant

$$\epsilon_0 = \frac{2\kappa}{\varpi \gamma_{\rm r}' \sqrt{\gamma_0}} \sqrt{\langle \hat{\sigma}_{\rm inv}^2 \rangle \langle \delta\hat{\sigma}(0)^2 \rangle - \langle \hat{\sigma}_{\rm inv} \delta\hat{\sigma}(0) \rangle^2},$$

in which $\delta\hat{\sigma}(0)$ can be replaced by $\hat{\sigma}(0)$. Equation (52) clearly shows that the correlated emittance is damped by $\sqrt{\gamma_{\rm r}}$ and periodically returns to zero, which is the behavior of an emittance-compensated beam [4]. External focusing controls the emittance oscillation through ϖ.

In a split photoinjector, a focused beam reaches a waist in the drift space before it diverges due to the repulsive space-charge forces. At the waist, $\hat{\sigma}' \propto \tau' = 0$, which is the same as the condition for matching a beam slice onto an invariant envelope in the booster. Therefore the beam waist is a natural location for the booster entrance. From Eqs. (32) and (41), all invariant envelopes match onto a single beam-spreading curve in τ with the matching condition $\tau_{\rm w} = \beta_{\rm r}\gamma_{\rm r}/\sqrt{\kappa} = 1/\sqrt{K^{\rm ext}}$, i.e.,

$$\left(\frac{\beta_{\rm r}\gamma_{\rm r}}{\tau_{\rm w}} \right)^2 = \frac{\kappa_{\rm s}}{\beta_{\rm r}\gamma_{\rm r}\sigma_{\rm w}^2} = \kappa \simeq \left(\frac{1}{4} + \frac{\eta}{8 \sin^2 \varphi_{\rm r}} \right) \langle \gamma' \rangle^2, \tag{53}$$

where the left-hand side is given by the parameters of the rms beam slice at the waist, and the right-hand side is determined by the booster field. These matching conditions have been shown to be effective [14].

Emittance evolution in the drift region of an optimized split injector has a double-minimum feature first observed in a simulation study of the Linac Coherent Light Source (LCLS) injector [16], which plays an important role in the design of split photoinjectors. This feature has been attributed to chromatic effects [14]. Although chromatic effects in the solenoid may contribute to the slice initial conditions at the beginning of the drift, the emittance oscillation in the drift is mainly due to beam spreading governed by Eq. (41). To demonstrate this, we analyzed a SPARC photoinjector design, which is similar to the LCLS injector design. At the beginning of the drift region, information about each slice was extracted from the HOMDYN [17] output, then Eq. (41) was used to numerically track the transverse evolution of all slices with the longitudinal profile frozen. The resulting emittance is plotted in Fig. 2 together with the HOMDYN result. Clearly the W-shaped emittance evolution is mainly due to beam spreading.

An analytical estimation of the emittance in (τ, τ') due to initial spread of τ_0 can be obtained from $|\tau \partial_{\tau_0} \tau' - \tau' \partial_{\tau_0} \tau| (\Delta\tau_0)_{\rm rms}$ (Appendix E). Taking the partial derivative of Eq. (44) with respect to τ_0 yields $\partial_{\tau_0}\tau = (\tau - \tau' s)/\tau_0$ and $\partial_{\tau_0}\tau' = -s/\tau_0\tau$. Thus the emittance estimation becomes

$$\epsilon = |W| \frac{(\Delta\tau_0)_{\rm rms}}{(\tau_0)_{\rm avg}}, \quad W = (\tau'^2 - 1)s - \tau\tau'. \tag{54}$$

From $W' = 2[(\tau'/\tau)s - 1] = 0$, we see that the function W has a minimum $W_{\rm min} = -s$ at $s = \tau/\tau'$. Therefore the emittance

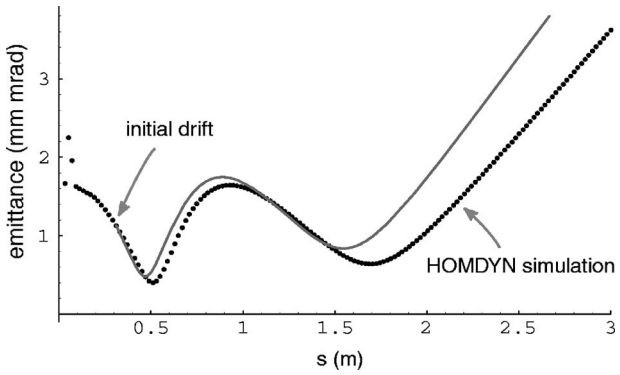

FIG. 2. Normalized rms emittance of a split-injector design. The dots are a HOMDYN simulation. The solid line is obtained by advancing slices extracted from HOMDYN through the drift space with Eq. (41), ignoring longitudinal evolution.

($\propto |W|$) has two minima where W crosses zero and one local maximum that is proportional to s, a result that shows the W-shaped emittance evolution. Figure 3 illustrates such an estimate for the case shown in Fig. 2. The gray curve is the function W calculated using τ from the numerical solution of Eq. (41) with initial values equal to the averages of the slices. The solid line is $|W|$. The dashed line is $|W|$ calculated with the approximate τ in Eq. (46). The dots are the emittance calculated by tracking individual slices, which has a large spread in τ_0' in addition to the spread in τ_0 that we are considering. The qualitative agreement confirms our understanding that the emittance oscillation is simply due to beam spreading of the slices, a generic feature of a space-charge-dominated beam in drift space. It is straightforward to improve the emittance estimation by taking into account the spread in τ_0', which is not pursued here since it is not essential for the understanding. (See [18] for further discussions.) Note that, in general, the emittance maxima are not located at the beam waist, which is the preferred location for matching the beam into a booster.

VI. THIRD-ORDER EFFECTS

In emittance-compensated injectors, all beam slices propagate close to their invariant envelopes with a small

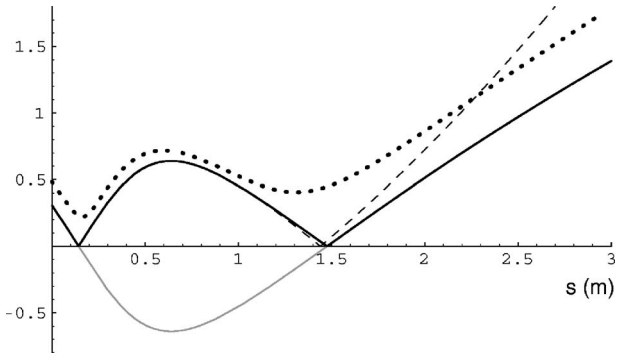

FIG. 3. Emittance in (τ, τ') normalized by $(\Delta\tau_0)_{\rm rms}/(\tau_0)_{\rm avg}$ for the case in Fig. 2 with the origin shifted to the beginning of the drift. The dots are tracking with Eq. (41). The solid line is the simple estimate given in Eq. (54). The dashed line is the same as the solid one but using the approximation in Eq. (46).

spread of phase-space angles around $\hat{\sigma}'_{\rm inv}/\hat{\sigma}_{\rm inv}=0$; thus all the terms involving transverse momentum are significantly smaller compared to the $\hat{x}^2+\hat{y}^2$ terms in the third-order Hamiltonian of Eq. (16), and will be neglected. Otherwise, there are many more terms than we would like to handle analytically here. Such a reduction in nonlinearity is another advantage to propagate slices around their invariant envelopes. Under such conditions, neglecting longitudinal dynamics, the third-order Hamiltonian Eq. (16) reduces to

$$H_3 \simeq \frac{(\hat{\phi}_0^{\rm sc})_3}{\hat{P}_{\rm r}^{\rm k}} + \frac{w_{\rm g}}{2\hat{P}_{\rm r}^{\rm k}}(\hat{x}^2+\hat{y}^2)\hat{z} - \frac{\beta_{\rm r}^2 w_{\rm c}}{2}(\hat{x}^2+\hat{y}^2)\delta_z, \quad (55)$$

where δ_z is the relative deviation of longitudinal kinematic momentum. In the chromatic term, $\hat{p}_z/\hat{P}_{\rm r}^{\rm k}=[p_z-(\partial_z\hat{A}_z)_{\rm r}\hat{z}]/\hat{P}_{\rm r}^{\rm k}=\delta_z+x_\perp\cdot(\nabla_\perp\hat{A}_z)_{\rm r}/\hat{P}_{\rm r}^{\rm k}+O(X^2)\simeq\delta_z$ has been used with $(\partial_\perp\hat{A}_z)_{\rm r}=0$. Since the longitudinal variables are treated as parameters in slice treatment, we replaced the canonical momentum $\hat{p}_z$ with δ_z. Assuming a longitudinally symmetric bunch, $\partial_z g(z,s)|_{\rm r}=0$; thus $(\hat{\phi}_0^{\rm sc})_3=0$, i.e., the space-charge potential does not contribute to the third order. However, space charges still contribute to the chromatic term through the vector potential $\hat{A}_z^{\rm sc}$ (contained in $\hat{A}_z$ without the "rf" superscript). Note that there is the possibility to cancel the geometric term due to the rf field with a longitudinally asymmetric bunch.

To evaluate the coefficients $w_{\rm c}$ and $w_{\rm g}$, we have, from the vector potential of the rf field in Eq. (17),

$$\left.\frac{\partial^2\hat{A}_r^{\rm rf}}{\partial z\,\partial r}\right|_{\rm r} = \frac{\hat{E}_0 c}{2\omega}\sum_{n=-\infty}^{\infty} a_n k_{zn}^2 e^{i\psi_n} \simeq \hat{E}_0 k\cos(ks)\cos(\varphi_{\rm r}+ks), \quad (56a)$$

$$\left.\frac{\partial^2\hat{A}_z^{\rm rf}}{\partial r^2}\right|_{\rm r} = -\frac{\hat{E}_0 c}{2\omega}\sum_{n=-\infty}^{\infty} a_n k_{rn}^2 e^{i\psi_n} \simeq 0, \quad (56b)$$

$$\left.\frac{\partial^3\hat{A}_z^{\rm rf}}{\partial z\,\partial r^2}\right|_{\rm r} = i\frac{\hat{E}_0 c}{2\omega}\sum_{n=-\infty}^{\infty} a_n k_{rn}^2 k_{zn} e^{i\psi_n} \simeq 0, \quad (56c)$$

where $\psi_n=\omega t(s)-k_{zn}s+\varphi_0$ is the rf phase of the reference particle and $\varphi_{\rm r}=\psi_0$ is referenced to the accelerating wave. In the approximations, we have assumed a π-mode standing wave with $a_0=a_{-1}=1$, $|k_{zn}|=k=\omega/c$, and $k_{rn}=0$. The coefficient $w_{\rm c}$ is similar to the linear focusing strength K in Eq. (21). With $\sqrt{\hat{P}_{\rm r}^{\rm k}}'/\sqrt{\hat{P}_{\rm r}^{\rm k}}=\sqrt{\beta_{\rm r}\gamma_{\rm r}}'/\sqrt{\beta_{\rm r}\gamma_{\rm r}}=\gamma'_{\rm r}/2\beta_{\rm r}^2\gamma_{\rm r}$ and $\partial_r^2\hat{A}_z^{\rm sc}/(\hat{P}_{\rm r}^{\rm k})^3=\partial_r^2\hat{\phi}_0^{\rm sc}/(\hat{P}_{\rm r}^{\rm k})^2=K^{\rm sc}=-2\kappa_{\rm s}/\beta_{\rm r}^3\gamma_{\rm r}^3\sigma_r^2$, we have

$$w_{\rm c}=\frac{1}{\beta_{\rm r}^2\gamma_{\rm r}^2}\left[\frac{\gamma_{\rm r}'^2}{4\beta_{\rm r}^2}+\left(\frac{qB_s}{2mc}\right)^2-\frac{2\kappa_{\rm s}}{\hat{\sigma}_r^2}+\frac{(\partial_r^2\hat{A}_z^{\rm rf})_{\rm r}}{\beta_{\rm r}\gamma_{\rm r}}\right]. \quad (57)$$

For slices propagating around their invariant envelopes, $\hat{\sigma}_r^2\simeq\kappa_{\rm s}/\kappa$, and thus

$$w_{\rm c}\simeq\frac{-1}{\beta_{\rm r}^2\gamma_{\rm r}^2}\left[\left(\frac{qB_s}{2mc}\right)^2+\frac{\eta}{4}\left(\frac{qE_0}{2mc^2}\right)^2+\frac{\gamma_{\rm r}'^2}{4}\right], \quad (58)$$

where the relativistic approximation is made in the $\gamma'_{\rm r}$ term, and $(\partial_r^2\hat{A}_z^{\rm rf})_{\rm r}\simeq 0$ is used. Inserting Eq. (56) in $w_{\rm g}$ we have

$$w_{\rm g}\simeq\alpha k^2\frac{\gamma'_{\rm r}}{\beta_{\rm r}^2\gamma_{\rm r}}\cos(ks)\cos(\varphi_{\rm r}+ks). \quad (59)$$

Here the constant $\alpha=\hat{E}_0/k=qE_0/2mc^2k$, as in [3].

Now let us estimate the magnitude of these nonlinear terms. For the chromatic term, we note that $w_{\rm c}\simeq -K^{\rm ext}$; thus the chromaticity is approximately -1, and the chromatic focusing is a factor δ_z weaker than the external focusing. For the rf geometric term, $|w_{\rm g}z/\beta_{\rm r}\gamma_{\rm r}K^{\rm ext}|\leqslant\alpha k^2\gamma'_{\rm r}\sigma_z/\beta_{\rm r}\kappa\sim\gamma_{\rm r}'^2\sigma_\varphi/\beta_{\rm r}\kappa=\sigma_\varphi/\beta_{\rm r}(\Omega^2+1/4)<4\sigma_\varphi/\beta_{\rm r}$, where σ_φ is the rf phase spread. Therefore, both the chromatic and rf corrections to the external focusing are typically less than a few percent (assuming $\beta_{\rm r}\simeq 1$). Since there are only a few emittance oscillations in a photoinjector, the overall phase spread in the envelope oscillations due to the slice-dependent external focusing is quite small. Nonetheless, they will contribute to the residual emittance by hindering perfect alignment of all slices.

To estimate this emittance degradation, we use the envelope solution Eq. (39) and consider the small variation in phase resulting from perturbations to the focusing strength κ and thus ϖ in u (other κ variations, such as in the initial amplitude, are neglected for simplicity). We consider the perfectly compensated case where all slices are aligned initially along $\hat{\sigma}'_r=0$ with $\theta=\theta_0$. Without nonlinear perturbations, the emittance evolution is given by Eq. (52). Assuming that the variation $\delta\kappa$ (due to energy spread or rf phase spread) is uncorrelated with the envelope deviation $\delta\hat{\sigma}_r$, the correction to the emittance can be estimated with $|\hat{\sigma}_r\partial_\kappa\hat{\sigma}'_r-\hat{\sigma}'_r\partial_\kappa\hat{\sigma}_r|(\delta\kappa)_{\rm rms}$. Inserting $\partial_\kappa\hat{\sigma}_r\simeq-\sqrt{\gamma_{\rm r}/\gamma_0}[\delta\hat{\sigma}_r(0)/\cos\theta_0]\sin(u+\theta_0)\partial_\kappa u$ and $\partial_\kappa\hat{\sigma}'_r\simeq-\sqrt{2\kappa/\gamma_0\gamma_{\rm r}}[\delta\hat{\sigma}_r(0)/\cos\theta_0]\cos(u)\partial_\kappa u$, we have

$$\begin{aligned}\Delta\epsilon &= \sqrt{\frac{2\kappa}{\gamma_0\gamma_{\rm r}}}\left|\frac{\delta\hat{\sigma}_r(0)}{\cos\theta_0}\left(\hat{\sigma}_{\rm inv}\cos u+\sqrt{\frac{\gamma_{\rm r}}{\gamma_0}}\delta\hat{\sigma}_r(0)\right)\frac{\partial u}{\partial\kappa}\right|(\delta\kappa)_{\rm rms}\\ &\simeq \sqrt{\frac{2\kappa}{\gamma_0\gamma_{\rm r}}}\left|\frac{u\cos u}{\cos\theta_0}\frac{1}{\varpi}\frac{\partial\varpi}{\partial\kappa}\right|(\hat{\sigma}_{\rm inv})_{\rm rms}[\delta\hat{\sigma}_r(0)]_{\rm rms}(\delta\kappa)_{\rm rms}\\ &= \frac{2\kappa(\hat{\sigma}_{\rm inv})_{\rm rms}[\delta\hat{\sigma}_r(0)]_{\rm rms}}{\varpi\gamma'_{\rm r}\sqrt{\gamma_0\gamma_{\rm r}}}\frac{(\delta\kappa)_{\rm rms}}{(\varpi\gamma'_{\rm r})^2}|u\cos u|, \end{aligned} \quad (60)$$

where the second term in large parentheses is dropped since it is much smaller than the first one when Eq. (39) holds. The first factor in this expression can be identified with $\epsilon_0/\sqrt{\gamma_{\rm r}}$ of Eq. (52) if $\langle\hat{\sigma}_{\rm inv}\delta\hat{\sigma}_r(0)\rangle$ can be neglected. The second factor is approximately $\delta\kappa/\kappa$, which is less than a few percent. For each emittance oscillation, u increases by π. Therefore, for a few emittance oscillations, this correction is much smaller than Eq. (52), and becomes significant only when $\sin u\simeq 0$ and $\cos u\simeq 1$ (especially when adding them quadratically). In other words, it contributes to the minimum emittance but does little to the overall emittance oscillation due to space

charge. Besides the factor $\cos u$, $\Delta\epsilon \propto \ln(\gamma_r/\gamma_0)/\sqrt{\gamma_0\gamma_r}$, which grows quickly to a maximum $2/e\gamma_0$ at $\gamma_r = e^2\gamma_0$ and then slowly decreases. Thus, replacing $u\cos u/\sqrt{\gamma_0\gamma_r}$ with ϖ/γ_0, we obtain the magnitude of $\Delta\epsilon \sim (2\kappa/\gamma_r')\sigma_0^2[\delta\hat{\sigma}_r(0)/\hat{\sigma}_{\rm inv}][\delta\kappa/(\varpi\gamma_r')^2]$. As an example, for a standing wave structure with $\gamma_r' = 100$, $\Omega^2 = 1/8$, initial rms beam size $\sigma_0 = 1$ mm, 10% envelope mismatch, and 1% κ variation, we have $\Delta\epsilon \sim 0.1$ mm mrad. However, things could be much worse if we loosen the parameters (especially in the early part of a photoinjector, where slices may be away from equilibrium).

Since the w_g term depends differently on s, the envelope solution Eq. (39) and the above treatment are inadequate. For a rough estimate, one might ignore the cosine factors or replace them with the slowly varying part $\cos\varphi_r/2$, which approaches zero if the final rf phase is $\pi/2$. We will not pursue this subject further here.

VII. CONCLUDING REMARKS

A general Hamiltonian suitable for perturbative analysis of rapidly accelerating beams is derived, which is mostly decoupled and has a familiar form. Based on the Hamiltonian, we presented a systematic and self-sufficient treatment of beam dynamics in rf photoinjectors. Our analysis provides an improved account of emittance-compensation theory. Efforts are made to point out various approximations used in the analysis for better understanding the limitations and for further improvements. Clearly, with an additional scalar potential [in Eq. (21) in particular] for the static electric field near the cathode, our analysis and emittance compensation apply to dc photoinjectors as well. Moreover, in addition to the solenoidal focusing considered in this paper, a sector of (skew) quadrupoles may be added to create a $\pi/2$ phase difference in the two transverse planes for generating a flat beam. It is straightforward to extend our analysis for such an injector as long as there is no overlap between the solenoids and quadrupoles. However, a magnetized beam with large angular momentum may not be space-charged dominated any longer. Further investigations are needed to incorporate transverse and longitudinal coupling and to address the question of minimum emittance achievable in such a system, which requires more adequate treatment of the nonrelativistic beam close to the cathode and better account of the emittance compensation process.

ACKNOWLEDGMENTS

The author is grateful to M. Ferrario for informative communications and more importantly for providing his code HOMDYN with the SPARC design example, which was used in this work. Furthermore, he would like to thank V. Kumar and J. Lewellen for helpful discussions and K.-J. Kim for encouragement to look into the dynamics of photoinjectors. This work is supported by the U.S. Department of Energy, Office of Basic Energy Sciences, under Contract No. W-31-109-ENG-38.

APPENDIX A: TERMS IN THE HAMILTONIAN

This appendix facilitates the calculations in Eqs. (7), (15), and (16).

The first-order term in Eq. (7) can be written as

$$
\begin{aligned}
H_1 &= \frac{1}{\beta_r}(\mathbf{x}\cdot\boldsymbol{\nabla}\hat{\phi})_r + \mathbf{x}\cdot\hat{\mathbf{P}}_r' - \mathbf{X}_r'\cdot\mathbf{p} + \hat{\mathbf{P}}_r^k\cdot\boldsymbol{\delta}_1 \\
&= -\mathbf{p}\cdot\left(\mathbf{X}_r' - \frac{\mathbf{P}_r^k}{P_r^k}\right) + \mathbf{x}\cdot\left(\hat{\mathbf{P}}_r' + \frac{q\,\boldsymbol{\nabla}\,\phi}{\beta_r mc^2}\right) - \frac{q\mathbf{v}_r\cdot(\Delta\mathbf{A})_1}{\beta_r mc^2} \\
&= \frac{\mathbf{x}}{\beta_r mc^2}\cdot[\dot{\mathbf{P}}_r + q\,\boldsymbol{\nabla}\,\phi - q\,\boldsymbol{\nabla}\,(\mathbf{v}_r\cdot\mathbf{A})] \\
&= \frac{\mathbf{x}}{\beta_r mc^2}\cdot\{\dot{\mathbf{P}}_r^k + q[\partial_t\mathbf{A} + \mathbf{v}_r\cdot\boldsymbol{\nabla}\mathbf{A} + \boldsymbol{\nabla}\phi - \boldsymbol{\nabla}(\mathbf{v}_r\cdot\mathbf{A})]\} \\
&= \frac{\mathbf{x}}{\beta_r mc^2}\cdot[\dot{\mathbf{P}}_r^k + q(\partial_t\mathbf{A} + \boldsymbol{\nabla}\phi) - q\mathbf{v}_r\times(\boldsymbol{\nabla}\times\mathbf{A})],
\end{aligned}
$$

where the overdot means d/dt and $\mathbf{v}_r$ is the velocity of the reference particle. All the differentiations are evaluated at the reference particle. We see that the vanishing of the first-order Hamiltonian is equivalent to vanishing of the square-bracket in the last expression, which is nothing but the Lorentz equation for the reference particle.

Terms in Eq. (15) can be calculated as follows. From $\boldsymbol{\delta} = (\mathbf{p} - \Delta\hat{\mathbf{A}})/\hat{P}_r^k$ and the canonical transformation in Eq. (13), we have

$$
\boldsymbol{\delta}_x = \frac{1}{\sqrt{\hat{P}_r^k}}\left\{\left[\hat{p}_x - \frac{\sqrt{\hat{P}_r^k}'}{\sqrt{\hat{P}_r^k}}\hat{x}\right] - \left[\frac{\Delta\hat{A}_x}{\sqrt{\hat{P}_r^k}} - \left(\frac{\partial_x\hat{A}_x}{\hat{P}_r^k}\right)_r\hat{x}\right]\right\},
$$

$$
\boldsymbol{\delta}_z = \frac{1}{\hat{P}_r^k}\{\hat{p}_z - [\Delta\hat{A}_z - (\partial_z\hat{A}_z)_r\hat{z}]\}.
$$

$\boldsymbol{\delta}_y$ can be obtained from $\boldsymbol{\delta}_x$ by switching x and y. The vector potential terms contain various orders. At the first order, with the field property $(\partial_z\hat{A}_\perp)_r = 0$, we have

$$
[\sqrt{\hat{P}_r^k}\Delta\hat{A}_x - (\partial_x\hat{A}_x)_r\hat{x}]_1 = (\partial_y\hat{A}_x)_r\hat{y},
$$

$$
[\Delta\hat{A}_z - (\partial_z\hat{A}_z)_r\hat{z}]_1 = \mathbf{x}_\perp\cdot(\boldsymbol{\nabla}_\perp\hat{A}_z)_r.
$$

Thus the first-order $\boldsymbol{\delta}$ becomes

$$
(\boldsymbol{\delta}_x)_1 = \frac{1}{\sqrt{\hat{P}_r^k}}\left\{\left[\hat{p}_x - \frac{\sqrt{\hat{P}_r^k}'}{\sqrt{\hat{P}_r^k}}\hat{x}\right] - \left(\frac{\partial_y\hat{A}_x}{\hat{P}_r^k}\right)_r\hat{y}\right\},
$$

$$
(\boldsymbol{\delta}_z)_1 = \frac{1}{\hat{P}_r^k}[\hat{p}_z - (\mathbf{x}_\perp\cdot\boldsymbol{\nabla}_\perp\hat{A}_z)_r].
$$

With these, the second-order kinematic term in the Hamiltonian becomes

$$\frac{\hat{P}_{\mathrm{r}}^{\mathrm{k}}}{2}\left(\boldsymbol{\delta}_{\perp}^2+\frac{1}{\gamma_{\mathrm{r}}^2}\boldsymbol{\delta}_z^2\right)_2$$
$$=\frac{\hat{p}_x^2}{2}-\frac{\sqrt{\hat{P}_{\mathrm{r}}^{\mathrm{k}}}'}{\sqrt{\hat{P}_{\mathrm{r}}^{\mathrm{k}}}}\hat{x}\hat{p}_x+\left(\frac{\sqrt{\hat{P}_{\mathrm{r}}^{\mathrm{k}}}'}{\sqrt{\hat{P}_{\mathrm{r}}^{\mathrm{k}}}}\right)^2\frac{\hat{x}^2}{2}$$
$$+\frac{\sqrt{\hat{P}_{\mathrm{r}}^{\mathrm{k}}}'}{\sqrt{\hat{P}_{\mathrm{r}}^{\mathrm{k}}}}\left(\frac{\partial_y\hat{A}_x}{\hat{P}_{\mathrm{r}}^{\mathrm{k}}}\right)_{\mathrm{r}}\hat{x}\hat{y}-\left(\frac{\partial_y\hat{A}_x}{\hat{P}_{\mathrm{r}}^{\mathrm{k}}}\right)_{\mathrm{r}}\hat{y}\hat{p}_x+\left(\frac{\partial_y\hat{A}_x}{\hat{P}_{\mathrm{r}}^{\mathrm{k}}}\right)_{\mathrm{r}}^2\frac{\hat{y}^2}{2}$$
$$+(x\leftrightarrow y)+\frac{1}{2\beta_{\mathrm{r}}\gamma_{\mathrm{r}}^3}[\hat{p}_z-(\mathbf{x}_{\perp}\cdot\boldsymbol{\nabla}_{\perp}\hat{A}_z)_{\mathrm{r}}]^2$$
$$=\frac{\hat{p}_x^2}{2}-\frac{\sqrt{\hat{P}_{\mathrm{r}}^{\mathrm{k}}}'}{\sqrt{\hat{P}_{\mathrm{r}}^{\mathrm{k}}}}\hat{x}\hat{p}_x+\left[\left(\frac{\sqrt{\hat{P}_{\mathrm{r}}^{\mathrm{k}}}'}{\sqrt{\hat{P}_{\mathrm{r}}^{\mathrm{k}}}}\right)^2+\left(\frac{\partial_x\hat{A}_y}{\hat{P}_{\mathrm{r}}^{\mathrm{k}}}\right)_{\mathrm{r}}^2\right]\frac{\hat{x}^2}{2}$$
$$+(x\leftrightarrow y\text{ in previous terms})+\left(\frac{\partial_y\hat{A}_x}{\hat{P}_{\mathrm{r}}^{\mathrm{k}}}\right)_{\mathrm{r}}(\hat{x}\hat{p}_y-\hat{y}\hat{p}_x)$$
$$+\frac{1}{2\beta_{\mathrm{r}}\gamma_{\mathrm{r}}^3}[\hat{p}_z-(\mathbf{x}_{\perp}\cdot\boldsymbol{\nabla}_{\perp}\hat{A}_z)_{\mathrm{r}}]^2.$$

The field property $(\partial_y\hat{A}_x)_{\mathrm{r}}=-(\partial_x\hat{A}_y)_{\mathrm{r}}$ has been used in the last step.

The canonical transformation results in extra second-order terms from the generating function F_2, which can be written as

$$\partial_s F_2=\frac{\sqrt{\hat{P}_{\mathrm{r}}^{\mathrm{k}}}'}{\sqrt{\hat{P}_{\mathrm{r}}^{\mathrm{k}}}}\hat{x}\hat{p}_x-\left[\frac{(\hat{P}_{\mathrm{r}}^{\mathrm{k}})''}{2\hat{P}_{\mathrm{r}}^{\mathrm{k}}}-\frac{1}{\hat{P}_{\mathrm{r}}^{\mathrm{k}}}\frac{\partial^2\hat{A}_x}{\partial s\partial x}\bigg|_{\mathrm{r}}\right]\frac{\hat{x}^2}{2}$$
$$+(x\leftrightarrow y)+\frac{\partial^2\hat{A}_z}{\partial s\partial z}\bigg|_{\mathrm{r}}\frac{\hat{z}^2}{2}.$$

The new second-order Hamiltonian in Eq. (15) is a combination of this with the above kinematic terms, as well as the potential terms. The coupling terms such as $\hat{x}\hat{p}_x$ are removed by design.

To evaluate the second-order potential terms and the third-order kinematic terms, we need the expression for the second-order vector potential $\hat{\mathbf{A}}_2$. For the field under consideration, given by Eqs. (17)–(19) we have

$$(\hat{A}_x)_2=\frac{1}{\sqrt{\hat{P}_{\mathrm{r}}^{\mathrm{k}}}}\left(\frac{\partial^2\hat{A}_r}{\partial z\partial r}\right)_{\mathrm{r}}\hat{x}\hat{z},\quad(\hat{A}_y)_2=\frac{1}{\sqrt{\hat{P}_{\mathrm{r}}^{\mathrm{k}}}}\left(\frac{\partial^2\hat{A}_r}{\partial z\partial r}\right)_{\mathrm{r}}\hat{y}\hat{z},$$

$$(\hat{A}_z)_2=\frac{(\partial_r^2\hat{A}_z)_{\mathrm{r}}}{\hat{P}_{\mathrm{r}}^{\mathrm{k}}}\frac{\hat{x}^2+\hat{y}^2}{2}+(\partial_z^2\hat{A}_z)_{\mathrm{r}}\frac{\hat{z}^2}{2}.$$

The transverse components are due to the rf field only while the longitudinal components are from rf and space charges.

The second-order potential terms in the Hamiltonian can be written as

$$\left(\frac{1}{\beta_{\mathrm{r}}}\hat{\phi}-\hat{A}_z\right)_2=\left(\frac{\hat{\phi}_0^{\mathrm{sc}}}{\beta_{\mathrm{r}}\gamma_{\mathrm{r}}}-\hat{A}_z^{\mathrm{ext}}\right)_2$$
$$=\frac{(\hat{\phi}_0^{\mathrm{sc}})_2}{\beta_{\mathrm{r}}\gamma_{\mathrm{r}}}-\left(\frac{\partial_r^2\hat{A}_z^{\mathrm{rf}}}{\hat{P}_{\mathrm{r}}^{\mathrm{k}}}\right)_{\mathrm{r}}\frac{\hat{x}^2+\hat{y}^2}{2}-(\partial_z^2\hat{A}_z^{\mathrm{rf}})_{\mathrm{r}}\frac{\hat{z}^2}{2}.$$

The third-order potential terms are

$$\left(\frac{1}{\beta_{\mathrm{r}}}\hat{\phi}-\hat{A}_z\right)_3=\left(\frac{\hat{\phi}_0^{\mathrm{sc}}}{\beta_{\mathrm{r}}\gamma_{\mathrm{r}}}-\hat{A}_z^{\mathrm{ext}}\right)_3,$$

where

$$(\hat{A}_z^{\mathrm{ext}})_3=(\partial_z^3\hat{A}_z^{\mathrm{rf}})_{\mathrm{r}}\frac{\hat{z}^3}{6}+\frac{1}{\hat{P}_{\mathrm{r}}^{\mathrm{k}}}\frac{\partial^3\hat{A}_z^{\mathrm{rf}}}{\partial z\partial r^2}\bigg|_{\mathrm{r}}\frac{(\hat{x}^2+\hat{y}^2)\hat{z}}{2}$$

is from the rf field.

The third-order kinematic term can be calculated, with $\boldsymbol{\delta}_2=-\hat{\mathbf{A}}_2/\hat{P}_{\mathrm{r}}^{\mathrm{k}}$ and the above expressions, as

$$\frac{\hat{P}_{\mathrm{r}}^{\mathrm{k}}}{2}\left(\boldsymbol{\delta}_{\perp}^2+\frac{1}{\gamma_{\mathrm{r}}^2}\boldsymbol{\delta}_z^2\right)_3=\hat{P}_{\mathrm{r}}^{\mathrm{k}}\left[(\boldsymbol{\delta}_{\perp})_1\cdot(\boldsymbol{\delta}_{\perp})_2+\frac{1}{\gamma_{\mathrm{r}}^2}(\boldsymbol{\delta}_z)_1(\boldsymbol{\delta}_z)_2\right]$$
$$=\frac{1}{\hat{P}_{\mathrm{r}}^{\mathrm{k}}}\left(\frac{\partial^2\hat{A}_r}{\partial z\partial r}\right)_{\mathrm{r}}$$
$$\times\left[\frac{\sqrt{\hat{P}_{\mathrm{r}}^{\mathrm{k}}}'}{\sqrt{\hat{P}_{\mathrm{r}}^{\mathrm{k}}}}(\hat{x}^2+\hat{y}^2)-(\hat{x}\hat{p}_x+\hat{y}\hat{p}_y)\right]\hat{z}$$
$$-\frac{1}{\beta_{\mathrm{r}}\gamma_{\mathrm{r}}^3}\left[\frac{(\partial_r^2\hat{A}_z)_{\mathrm{r}}}{\hat{P}_{\mathrm{r}}^{\mathrm{k}}}\frac{\hat{x}^2+\hat{y}^2}{2}+(\partial_z^2\hat{A}_z)_{\mathrm{r}}\frac{\hat{z}^2}{2}\right]\hat{p}_z.$$

Here we have assumed $(\boldsymbol{\nabla}_{\perp}A_z)_{\mathrm{r}}=0$, i.e., there is no transverse dipole field.

APPENDIX B: SPACE-CHARGE POTENTIAL

Here we present a brief overview of the space-charge potential considered in this work following [19]. For an ellipsoidal symmetric bunch with charge density

$$\rho_{\mathrm{e}}(x,y,z)=\int_0^{\infty}ds\,f(s)\delta\left(s-\frac{x^2}{a^2}-\frac{y^2}{b^2}-\frac{z^2}{c^2}\right),\qquad\text{(B1)}$$

where f is some density profile, the scalar potential can be written as [19]

$$\phi(x,y,z)=-\frac{abc}{4\varepsilon_0}\int_0^{\infty}\frac{dt}{R(t)}\int_0^{S(t)}ds\,f(s),\qquad\text{(B2)}$$

with

$$R(t)=\sqrt{(t+a^2)(t+b^2)(t+c^2)},$$

$$S(t)=\frac{x^2}{a^2+t}+\frac{y^2}{b^2+t}+\frac{z^2}{c^2+t}.$$

Expanding ϕ around the axis $x=y=0$ to the third order, we have

$$\phi = -\frac{abc}{4\varepsilon_0}\int_0^\infty \frac{dt}{R(t)}\left[\int_0^{z^2/(c^2+t)} f(s)ds + \frac{f\left(\frac{z^2}{c^2+t}\right)}{a^2+t}x^2 + \frac{f\left(\frac{z^2}{c^2+t}\right)}{b^2+t}y^2 + \cdots\right]. \tag{B3}$$

There are no odd-order terms due to symmetry.

For an axisymmetric Gaussian bunch of charge Q, rms width σ_r, and length σ_z,

$$f(s) = \frac{Q}{\pi^{3/2}abc}e^{-s} \quad \text{with } a^2 = b^2 = 2\sigma_r^2, \quad c^2 = 2\sigma_z^2.$$

The scalar potential becomes

$$\phi = -\frac{Q}{4\pi\varepsilon_0\sqrt{2\pi}\sigma_z}\left[g_0 + g\frac{x^2+y^2}{2\sigma_r^2} + O(X^4)\right], \tag{B4}$$

where

$$g_0(z) = \int_0^\infty d\xi \frac{1-e^{-z^2/2\sigma_z^2(1+A^2\xi)}}{(1+\xi)\sqrt{1+A^2\xi}},$$

$$g(z) = \int_0^\infty d\xi \frac{e^{-z^2/2\sigma_z^2(1+A^2\xi)}}{(1+\xi)^2\sqrt{1+A^2\xi}},$$

and $A=a/c=\sigma_r/\sigma_z$ is the bunch aspect ratio. Note that g is the same geometric form factor as in [4]. When applied to the beam frame, σ_z should be replaced by $\gamma_r\sigma_z$ due to the relativistic effect.

For a uniformly distributed ellipsoidal bunch (water-bag model with constant f inside), Eq. (B2) is clearly a linear function of x^2, y^2, and z^2 inside the bunch with constant coefficients along the bunch. Thus, the space-charge force is completely linear and has the same transverse defocusing strength for all slices, which is ideal for preserving beam emittance and getting around emittance compensation. More explicitly, $f(s)=3Q/4\pi abc$ inside the ellipsoid, and, for the axisymmetric bunch with $a=b$,

$$\phi_{\text{inside}} = -\frac{3Q}{16\pi\varepsilon_0 c}\left(g_0 + g\frac{x^2+y^2}{a^2}\right), \tag{B5}$$

where

$$g_0 = \int_0^\infty \frac{(z^2/c^2)d\xi}{(1+\xi)(1+A^2\xi)^{3/2}}, \quad g = \int_0^\infty \frac{d\xi}{(1+\xi)^2\sqrt{1+A^2\xi}}.$$

These integrals can be worked out. Setting $c\to\infty$ gives $g_0=0$, $g=1$, and the expected simple potential inside a uniform cylinder beam $\phi=-(\lambda/4\pi\varepsilon_0)(x^2+y^2)/a^2$. The line charge density λ relates to Q via $Q=4\lambda c/3$.

We see that, with proper form factors, Eq. (19) covers, either exactly or as third-order approximations, most bunch models considered in photoinjectors.

APPENDIX C: SMOOTHED RF FOCUSING

The transverse Lorentz force due to the rf field is given by

$$F_r = q(\mathbf{E}+\mathbf{v}\times\mathbf{B}) = q(E_r - v_z B_\theta) = (\partial_r F_r)_{\mathrm{r}} r + \cdots, \tag{C1}$$

where

$$\begin{aligned}(\partial_r F_r)_{\mathrm{r}} &= q\partial_r[-\partial_t A_r - \beta_{\mathrm{r}} c(\partial_z A_r - \partial_r A_z)] \\ &= q\beta_{\mathrm{r}} c\partial_r[(\partial_z - \partial_s)A_r - (\partial_z A_r - \partial_r A_z)] \\ &= -\beta_{\mathrm{r}} mc^2(\partial_s\partial_r\hat{A}_r - \partial_r^2\hat{A}_z)_{\mathrm{r}}.\end{aligned} \tag{C2}$$

Therefore, the second term in Eq. (21) represents the transverse Lorentz force. It usually contains fast rf oscillations. The average Lorentz force has been studied [5,6] and referred to as "ponderomotive focusing," which is a second-order effect. Note that the Lorentz focusing expressions used in both references are not quite right.

In reduced coordinates, in addition to the Lorentz force, there is a pseudofocusing, Eq. (22), due to acceleration. Surprisingly, its leading term results from γ_{r}'' and cancels the Lorentz focusing exactly. To show this, i.e., Eq. (24), we start from Eq. (23) and using the Coulomb gauge condition $\nabla\cdot\mathbf{A}=0$ and the wave equation $[\nabla^2-(1/c^2)\partial_t^2]A_z=0$. For the reference particle, these two conditions yields $2\partial_r A_r+\partial_z A_z=0$ and $[2\partial_r^2+\partial_z^2-(1/c^2)\partial_t^2]A_z=0$, respectively. Thus

$$\begin{aligned}\gamma_{\mathrm{r}}'' &= \left(\frac{1}{\beta c}\partial_t + \partial_z\right)\gamma_{\mathrm{r}}' = -\frac{1}{\beta c^2}\partial_t^2\hat{A}_z + \partial_z[\beta(\partial_z-\partial_s)\hat{A}_z] \\ &= -\frac{1}{\beta c^2}\partial_t^2\hat{A}_z + \beta\left(\frac{1}{c^2}\partial_t^2 - 2\partial_r^2\right)\hat{A}_z + 2\beta\partial_s\partial_r\hat{A}_r \\ &= -\frac{1}{\beta\gamma^2 c^2}\partial_t^2\hat{A}_z + 2\beta(\partial_s\partial_r\hat{A}_r - \partial_r^2\hat{A}_z).\end{aligned} \tag{C3}$$

All quantities are for the reference particle. The last term will cancel the Lorentz focusing. Thus the total rf focusing is given by the residual pseudofocusing Eq. (25).

Now let us compute the average focusing strength in Eq. (26). From Eq. (17) the longitudinal rf field seen by the reference particle is

$$\hat{E}_z = -\frac{1}{c}\partial_t\hat{A}_z = \mathrm{Im}\left(\hat{\mathsf{E}}_0\sum_{n=-\infty}^{\infty} a_n e^{i\psi_n}\right) = \hat{\mathsf{E}}_0\sum_{n=-\infty}^{\infty} a_n \sin\psi_n, \tag{C4}$$

where the phase for the nth spatial harmonic $\psi_n=\omega t(s)-k_{zn}s+\varphi_0=-2nk_0 s+\omega t-k_0 s+\varphi_0=-2nk_0 s+\varphi_{\mathrm{r}}$, and k_0 is the wave number of the fundamental accelerating wave. For synchronized acceleration, φ_{r} is roughly constant (at relativistic energy); thus the average longitudinal field and its time derivative become

$$\langle\hat{E}_z\rangle \simeq \hat{\mathsf{E}}_0\sin\varphi_{\mathrm{r}} \quad \text{and} \quad \langle\partial_t\hat{E}_z\rangle \simeq \omega\hat{\mathsf{E}}_0\cos\varphi_{\mathrm{r}}. \tag{C5}$$

Note that in our normalization $a_0=1$, corresponding to the fundamental accelerating wave. The square of the field can be averaged as

$$\langle \hat{E}_z^2 \rangle = \hat{\mathsf{E}}_0^2 \sum_{m,n=-\infty}^{\infty} a_m a_n \langle \sin\psi_m \sin\psi_n \rangle$$
$$\simeq \hat{\mathsf{E}}_0^2 \sum_{n=-\infty}^{\infty} \frac{1}{2}(a_n^2 - a_n a_{-n}\cos 2\varphi_r) = \hat{\mathsf{E}}_0^2\left(\sin^2\varphi_r + \frac{\eta}{2}\right), \tag{C6}$$

where

$$\eta \equiv \sum_{n=1}^{\infty}(a_n^2 + a_{-n}^2 - 2a_n a_{-n}\cos 2\varphi_r)$$
$$= \sum_{n=0}^{\infty}(a_n^2 + a_{n+1}^2 - 2a_n a_{n+1}\cos 2\varphi_r). \tag{C7}$$

The last expression is for a standing wave structure with $a_{-(n+1)}=a_n^*$. The amplitudes of the space harmonics are assumed to be real, i.e., the origin is located at a symmetric point of the rf structure. Insert Eqs. (C6) and (C5) into the average of Eq. (25), which yields the smoothed rf focusing strength Eq. (26), assuming β_r and γ_r can be replaced with their averaged values and taken out of the average.

To relate better to the expressions in the literature, especially [4–6], here we give the on-axis electric field and focusing strength expressions using a different labeling. For a π-mode standing wave structure, Eq. (C4) can be written as

$$E_z = \mathsf{E}_0\,\mathrm{Im}\left(\sum_{n=-\infty}^{\infty} a_n e^{i(-2nks+\varphi_r)}\right)$$
$$= 2\mathsf{E}_0\,\mathrm{Im}\left(\sum_{n=0}^{\infty} a_n e^{i(ks+\varphi_r)}\cos(2n+1)ks\right)$$
$$= E_0\sum_{n=0}^{\infty} a_n \cos[(2n+1)ks]\sin(ks+\varphi_r). \tag{C8}$$

Note that the amplitude of the accelerating electric field $E_0 = 2\mathsf{E}_0$, i.e., twice the amplitude of the fundamental harmonic because the forward and backward waves may add up constructively. The normalized field amplitude reads (note the extra factor of 2)

$$\hat{E}_0 \equiv \frac{q\mathsf{E}_0}{mc^2} = \frac{qE_0}{2mc^2} = \alpha k, \tag{C9}$$

where α is the dimensionless field strength used in [3].

Relabeling the coefficients with $\mathsf{a}_n = a_{(n-1)/2}$, we can write the electric field as

$$E_z = E_0 \sum_{n=\mathrm{odd}} \mathsf{a}_n \cos(nks)\sin(ks+\varphi_r), \tag{C10}$$

and the η in smoothed ponderomotive focusing as

$$\eta = \sum_{n=\mathrm{odd}} (\mathsf{a}_n^2 + \mathsf{a}_{n+2}^2 - 2\mathsf{a}_n\mathsf{a}_{n+2}\cos 2\varphi_r). \tag{C11}$$

These are the same as in [4,5], except for a different reference phase in [4], provided that $\mathsf{a}_n = 0$ for even n.

APPENDIX D: TRANSFER MATRIX OF A RF CAVITY

For a relativistic particle passing through a TM_{01}-mode rf cavity, from Eqs. (20), (27), and (29),

$$\hat{x}'' + \frac{\kappa}{\gamma^2}\hat{x} = 0, \quad \kappa = \gamma'^2\left(\frac{1}{4} + \frac{\eta}{8\sin^2\varphi_r}\right). \tag{D1}$$

Hereafter subscripts referring to the reference particle are dropped. One way to solve this homogeneous differential equation is to seek independent solutions of the form γ^λ. It is more interesting to turn the equation of motion into

$$\frac{d^2x}{du^2} + x = 0, \tag{D2}$$

by using $u \equiv \varpi \ln(\gamma/\gamma_0)$ with $\gamma'' \simeq 0$ under the smooth approximation, where

$$\varpi \equiv \sqrt{\frac{\kappa}{\gamma'^2} - \frac{1}{4}} = \sqrt{\eta/8\sin^2\varphi_r}, \tag{D3}$$

and γ_0 is an initial energy. The solution is a rotation

$$\begin{bmatrix} x \\ \dot{x} \end{bmatrix} = \begin{bmatrix} \cos u & \sin u \\ -\sin u & \cos u \end{bmatrix}\begin{bmatrix} x_0 \\ \dot{x}_0 \end{bmatrix}. \tag{D4}$$

Here the overdot stands for d/du. Since $\hat{p} = \hat{x}' = \sqrt{\gamma}'x + \sqrt{\gamma}x' = (\gamma'/\sqrt{\gamma})(x/2 + \varpi\dot{x})$, the transformation between the coordinates is

$$\begin{bmatrix} x \\ \dot{x} \end{bmatrix} = \begin{bmatrix} \dfrac{1}{\sqrt{\gamma}} & 0 \\ \dfrac{-1}{2\varpi\sqrt{\gamma}} & \dfrac{\sqrt{\gamma}}{\varpi\gamma'} \end{bmatrix}\begin{bmatrix} \hat{x} \\ \hat{p} \end{bmatrix}. \tag{D5}$$

Thus, through a similarity transformation, the transfer matrix in $(\hat{x},\hat{p})$ becomes

$$\begin{bmatrix} \sqrt{\dfrac{\gamma}{\gamma_0}}\left(\cos u - \dfrac{1}{2\varpi}\sin u\right) & \dfrac{\sqrt{\gamma_0\gamma}}{\varpi\gamma'}\sin u \\ -\dfrac{\varpi\gamma'}{\sqrt{\gamma_0\gamma}}\left(1 + \dfrac{1}{4\varpi^2}\right)\sin u & \sqrt{\dfrac{\gamma_0}{\gamma}}\left(\cos u + \dfrac{1}{2\varpi}\sin u\right) \end{bmatrix}. \tag{D6}$$

It is valid inside and outside a cavity with hard-edge fringe, i.e., there are no extra kicks, since the canonical coordinates are continuous across the edges (impulse approximation).

To see that it is the same transfer matrix as in [6], note that, outside the cavity $(\hat{x},\hat{p}) = \sqrt{\gamma}(x,x')$; thus by scaling the canonical transfer matrix with $\sqrt{\gamma_i}$ at the entrance with initial energy $\gamma_i = \gamma_0$ and with $1/\sqrt{\gamma_f}$ at the exit with final γ_f, we have the transfer matrix in (x,x') as

$$\begin{bmatrix} \cos u - \frac{1}{2\varpi}\sin u & \frac{\gamma_i}{\varpi\gamma'}\sin u \\ -\frac{\varpi\gamma'}{\gamma_f}\left(1+\frac{1}{4\varpi^2}\right)\sin u & \frac{\gamma_i}{\gamma_f}\left(\cos u + \frac{1}{2\varpi}\sin u\right) \end{bmatrix}, \tag{D7}$$

which is the same as Eq. (13) of [6] except for a couple of apparent typos. Note that it is more complicated to cross edges in (x,x'). At the inside and outside of the edges, $\hat{x}' = \sqrt{\beta\gamma}' x + \sqrt{\beta\gamma}\, x'_{\text{in}} = \sqrt{\beta\gamma}\, x'_{\text{out}}$; thus x' must experience an impulse kick of magnitude $\sqrt{\beta\gamma}' x/\sqrt{\beta\gamma} = (\gamma'/2\beta^2\gamma)x \simeq (\gamma'/2\gamma)x$ to cross an edge. It is negative at the entrance and positive at the exit. In other words, there are fringe matrices in (x,x') that read

$$\begin{bmatrix} 1 & 0 \\ -\gamma'/2\gamma_i & 1 \end{bmatrix} \quad \text{and} \quad \begin{bmatrix} 1 & 0 \\ \gamma'/2\gamma_f & 1 \end{bmatrix} \tag{D8}$$

at the entrance and the exit, respectively.

Clearly, the evolution of the envelope deviation, Eq. (38), is also given by the same transfer matrix Eq. (D6) with

$$\varpi = \sqrt{\frac{2\kappa}{\gamma'^2} - \frac{1}{4}} = \sqrt{2\Omega^2 + \frac{1}{4}}. \tag{D9}$$

From the transfer matrix, we can write

$$\begin{aligned} \delta\hat{\sigma}_r &= \sqrt{\frac{\gamma}{\gamma_0}}\delta\hat{\sigma}_r(0)\left[\cos u - \left(\frac{1}{2\varpi} - \frac{\gamma_0\delta\hat{\sigma}'_r(0)}{\varpi\gamma'\,\delta\hat{\sigma}_r(0)}\right)\sin u\right] \\ &= \sqrt{\frac{\gamma}{\gamma_0}}\frac{\delta\hat{\sigma}_r(0)}{\cos\theta}\cos(u+\theta), \end{aligned} \tag{D10}$$

where the symbols are defined as before. $\delta\hat{\sigma}'_r$ can be obtained similarly or by differentiating the above expression.

APPENDIX E: EMITTANCE CALCULATION

First of all, clearly the rms emittance computed with the reduced coordinates is the normalized emittance in phase space, which is conserved during acceleration if all the forces are linear.

In the laminar regime, the rms emittance ϵ of a bunch can be computed via

$$\epsilon = \sqrt{\langle\hat{\sigma}^2\rangle\langle\hat{\sigma}'^2\rangle - \langle\hat{\sigma}\hat{\sigma}'\rangle^2}, \tag{E1}$$

where the angular brackets mean averaging over the slices in a bunch. In general, such a computation could be rather messy [18]. To obtain a simple approximation, we linearize the dependence on, say, current around the peak current I_p, as $\hat{\sigma}(I) \simeq \hat{\sigma}(I_p) + \partial_I\hat{\sigma}\,\delta I$ and $\hat{\sigma}'(I) \simeq \hat{\sigma}'(I_p) + \partial_I\hat{\sigma}'\,\delta I$, with which the emittance can be expressed as

$$\epsilon = |\hat{\sigma}\partial_I\hat{\sigma}' - \hat{\sigma}'\partial_I\hat{\sigma}|_{I_p}\widehat{\delta I} = \hat{\sigma}(I_p)^2\left|\frac{\partial}{\partial I}\left(\frac{\hat{\sigma}'}{\hat{\sigma}}\right)\right|_{I_p}\widehat{\delta I}, \tag{E2}$$

where $\widehat{\delta I}$ stands for the standard deviation from I_p. Note that this approximation is the same as the commonly used two-slice emittance

$$\epsilon = \frac{1}{2}|\hat{\sigma}_+\hat{\sigma}'_- - \hat{\sigma}_-\hat{\sigma}'_+| = \frac{\beta\gamma}{2}|\sigma_+\sigma'_- - \sigma_-\sigma'_+|, \tag{E3}$$

provided that we let $\hat{\sigma}_+ = \hat{\sigma}_{I_p}$ and $\hat{\sigma}_- = \hat{\sigma}_{I_p} + \partial_I\hat{\sigma}\Delta I$, i.e., $\partial_I\hat{\sigma} = (\hat{\sigma}_- - \hat{\sigma}_+)/\Delta I$ and $\widehat{\delta I} = \Delta I/2$.

[1] B. E. Carlsten, Nucl. Instrum. Methods Phys. Res. A **285**, 313 (1989).
[2] X. Qiu, K. Batchelor, I. Ben-Zvi, and X.-J. Wang, Phys. Rev. Lett. **76**, 3723 (1996).
[3] K. J. Kim, Nucl. Instrum. Methods Phys. Res. A **275**, 201 (1989).
[4] L. Serafini and J. B. Rosenzweig, Phys. Rev. E **55**, 7565 (1997).
[5] S. C. Hartman and J. B. Rosenzweig, Phys. Rev. E **47**, 2031 (1993).
[6] J. Rosenzweig and L. Serafini, Phys. Rev. E **49**, 1599 (1994).
[7] F. Zimmermann and T. Raubenheimer, Nucl. Instrum. Methods Phys. Res. A **390**, 279 (1997).
[8] See, for example, J. D. Lawson, *The Physics of Charged Particle Beams*, 2nd ed. (Oxford University Press, New York, 1988).
[9] P. Lapostolle, E. Tanke, and S. Valero, Part. Accel. **44**, 215 (1994).
[10] E. D. Courant and H. S. Snyder, Ann. Phys. (N.Y.) **3**, 1 (1958).
[11] C.-X. Wang, Nucl. Instrum. Methods Phys. Res. A **557**, 94 (2006).
[12] See, for example, S. Y. Lee, *Accelerator Physics* (World Scientific, Singapore, 1999).
[13] See, for example, M. Reiser, *Theory and Design of Charged Particle Beams* (Wiley & Sons, New York, 1994).
[14] M. Ferrario *et al.*, *Physics and Applications of High Brightness Electron Beams* (World Scientific, Singapore, 2003).
[15] L. Brillouin, Phys. Rev. **67**, 260 (1945).
[16] M. Ferrario, J. E. Clendenin, D. T. Palmer, J. B. Rosenzweig, and L. Serafini, Report No. SLAC-PUB-8400, 2000 (unpublished).
[17] M. Ferrario and L. Serafini, in Proceedings of the Sixth European Particle Accelerator Conference (EPAC'98), 1999, http://accelconf.web.cern.ch/accelconf/
[18] C.-x. Wang, in Proceedings of the 35th Advanced ICFA Beam Dynamics Workshop on Physics and Application of High-Brightness Electron Beams, 2005 (to be published).
[19] R. L. Gluckstern, Fermilab Tech Note No. TM-1402, 1986 (unpublished).